frontiers | Frontiers in Nanotechnology

TYPE Review
PUBLISHED 24 August 2022
DOI 10.3389/fnano.2022.978358

OPEN ACCESS

EDITED BY
Marco Aurélio Suller Garcia,
Federal University of Maranhão, Brazil

REVIEWED BY
Yuechang Wei,
China University of Petroleum, Beijing, China
Dedong He,
Kunming University of Science and Technology, China

*CORRESPONDENCE
Eduardo Falabella Sousa-Aguiar,
efalabella@eq.ufrj.br

SPECIALTY SECTION
This article was submitted to Nanocatalysis, a section of the journal Frontiers in Nanotechnology

RECEIVED 25 June 2022
ACCEPTED 01 August 2022
PUBLISHED 24 August 2022

CITATION
Tavares M, Westphalen G, Araujo Ribeiro de Almeida JM, Romano PN and Sousa-Aguiar EF (2022), Modified fischer-tropsch synthesis: A review of highly selective catalysts for yielding olefins and higher hydrocarbons. *Front. Nanotechnol.* 4:978358. doi: 10.3389/fnano.2022.978358

Modified fischer-tropsch synthesis: A review of highly selective catalysts for yielding olefins and higher hydrocarbons

Marlon Tavares[1], Gisele Westphalen[1], João Monnerat Araujo Ribeiro de Almeida[2], Pedro Nothaft Romano[3] and Eduardo Falabella Sousa-Aguiar[1]*

[1]Escola de Química, Universidade Federal do Rio de Janeiro, Rio de Janeiro, Brazil, [2]Instituto de Química, Universidade Federal do Rio de Janeiro, Rio de Janeiro, Brazil, [3]Campus Duque de Caxias, Universidade Federal do Rio de Janeiro, Rio de Janeiro, Brazil

Global warming, fossil fuel depletion, climate change, as well as a sudden increase in fuel price have motivated scientists to search for methods of storage and reduction of greenhouse gases, especially CO_2. Therefore, the conversion of CO_2 by hydrogenation into higher hydrocarbons through the modified Fischer–Tropsch Synthesis (FTS) has become an important topic of current research and will be discussed in this review. In this process, CO_2 is converted into carbon monoxide by the reverse water-gas-shift reaction, which subsequently follows the regular FTS pathway for hydrocarbon formation. Generally, the nature of the catalyst is the main factor significantly influencing product selectivity and activity. Thus, a detailed discussion will focus on recent developments in Fe-based, Co-based, and bimetallic catalysts in this review. Moreover, the effects of adding promoters such as K, Na, or Mn on the performance of catalysts concerning the selectivity of olefins and higher hydrocarbons are assessed.

KEYWORDS

modified fischer-tropsch synthesis, carbon dioxide, reverse water-gas-shift reaction, olefins, higher hydrocarbons

Introduction

Due to the growing world demand for fuels and, at the same time, the need to reduce the greenhouse gas concentration in the atmosphere, the conversion of CO_2 into hydrocarbons via hydrogenation have gained considerable importance among scientists.

The hydrogenation of CO_2 into hydrocarbons in the liquid fuel range can be obtained via a methanol-mediated process or a modified Fischer-Tropsch Synthesis (FTS). In the first route, CO_2 is converted to methanol, then transformed into hydrocarbons through the commercially available methanol-to-gasoline (MTG) process based on zeolite catalysts (Wang et al., 2016; Gao et al., 2017; Sedighi and Mohammadi, 2020). The modified FTS also proceeds by a two-step process with the initial conversion of CO_2 into

TABLE 1 Production of hydrocarbons in cobalt, iron, and bimetallic catalysts.

Catalyst Conditions			Selectivity (%)						Reaction Conditions			
Metal	Support	Particle Size (nm)	X_{CO2}	CO	CH_4	C_2-C_4	C_2-$C_4^=$	C_{5+}	H_2/CO_2	T (°C)	P (MPa)	Ref
Co	Ceo		7.0		6.4				25/1	260	0.1	Das and Deo, (2012a)
	TiO_2		37		87.0	13.0			3/1	220	2.0	Yao et al. (2012)
	Al_2O_3	91	76	17.8	82.2				10/1	270	0.1	Srisawad et al. (2012)
	MIL-53(Al)		37.5	3.3	53.2	24.1		22.7	27/10	340	3.0	Tarasov et al. (2018a)
	Nb_2O_5	4–6	100		100				5/2	320	1.0	Tursunov and Tilyabaev, (2019)
		28.5	73.0	2.0	98.0				4/1	230	1.0	Jimenez et al. (2019)
	SiO_2		57.0	10.5	100				5/1	350	0.1	Garbarino et al. (2020)
	Al_2O_4	4.9	45.0	18.0	100				3/1	400	2.0	Kim et al. (2020a)
	SiO_2		11.0	96.0	100				4/1	550	1.0	Jimenez et al. (2020)
Fe	SiO_2		25.7	5.7	65.7	32.2		2.1	3/1	370	0.1	Owen et al. (2013a)
	CNT		32.2	16.1	56.6	37.9		5.5	3/1	370	0.8	Minett et al. (2014)
	OCNT		35.2	26.3	52.7	44.7		2.6	3/1	360	2.5	Chew et al. (2014a)
	NCNT	21–24	25.2	35.6	63.5	34.9		1.6	3/1	360	2.5	Chew et al. (2014b)
	Fe_3O_4	12				30.0		70	1/1		0.1	Wang et al. (2014)
	CeO_2		20.6	61.2	80.6	6.2	12.3	0.6	3/1	390		Torrente-Murciano et al. (2016)
	C		21.9	78.3	50.5	46.3		3.2	2/1	370	0.1	Gupta et al. (2016)
	Mo_2C			6.8	43.5	56.5			3/1	200	4.0	Chen et al. (2016)
	CT	75	40.0	15.0	14.1	43.5		42.4	3/1	350	1.5	Albrecht et al. (2017)
			46.0	17.5	26.6	14.5	19.2	22.2	3/1	400	3.0	Liu et al. (2017)
	NC		28.0	17.8	32.6	15.3	25.8	26.3	3/1	320	3.0	Liu et al. (2019)
	C-PYL	3	21.6	29.2	36.8	46.0		17.2	3/1	300	1.0	Guo et al. (2019)
	CNT		20.0	22.0	46.2	42.3		11.5	2/1	350	8.5	Chernyak et al. (2020)
			13.6	22.2	32.1	30.7		37.1[a]	2/1	230	1.6	Chen et al. (2020)
			34.1	12.6	13.0	40.3		46.7	3/1	320	3.0	Yao et al. (2021)
		27–29	23.5	40.9	14.6	85.4			3/1	300	1.5	Skrypnik et al. (2021)
		9.2	41.7	13.0	19.5	16.7	28.2	35.6	3/1	320	3.0	Liu et al. (2021a)
	MgO-Al_2O_3	16.6	50.1	20.3	47.1	46.6		6.3	4/1	275	0.2	Li et al. (2021)
Fe-Cu			16.7	31.4	2.4	32.7		64.9	3/1	300	1.0	Choi et al. (2017a)
Ni-Ru	BMI·NTf2 IL	2–3	30.0		5.0	76.0	16.0	3.0[b]	4/1	150	0.9	Qadir et al. (2019)
Fe-Co	Al_2O_3		4.9		4.7				25/1	260	0.1	Das and Deo, (2012b)
	NC		37.0	1.1	47.4	22.1	28.8	1.7	3/1	350	2.0	Dong et al. (2020)
	C	4,000	34.9	9.3	57.1	37.5		5.4		300	1.0	Cui et al. (2021)

= : olefinic products; [a]: C_5; b: C_5-C_6.

CO by the reverse water gas shift (RWGS), followed by hydrogenation of carbon monoxide into hydrocarbons by regular FTS (Geng et al., 2016), as follows.

$$CO_2 + H_2 \rightarrow CO + H_2O \quad \Delta H_{573K} = 38 kJ\ mol^{-1} \qquad (1)$$

$$CO + 2H_2 \rightarrow (1/n)(C_nH_{2n}) \quad \Delta H_{573K} = -166 kJmol^{-1} \qquad (2)$$

In the RWGS reaction, CO is obtained through CO_2 conversion to form *CO precursor molecules adsorbed on the catalyst surface. The product distribution can be broad, and changes depending on the catalysts' structure and composition. Thus, it is necessary to prevent high selectivity to methane and light-saturated hydrocarbons (Martinelli et al., 2014; Visconti et al., 2016).

Like the regular FTS, Fe-based, Co-based, and bimetallic catalysts have been extensively used to catalyze the CO_2 hydrogenation to C_{2+} hydrocarbons (Khodakov et al., 2007; Díaz et al., 2014). The iron catalysts have activity for both the RWGS and FTS reactions. Cobalt is already widely used in the industry for the regular FTS, and bimetallic catalysts like Fe-Co combine the properties of each metal with improving the catalytic performance. To improve the catalysts' hydrocarbon selectivity and reaction activity, the use of specific supports and the addition of promoters are common approaches. Therefore, a detailed discussion will focus on recent developments in catalyst design and catalytic performance, such as the effects of promoters and supports on yields and selectivity of hydrocarbons.

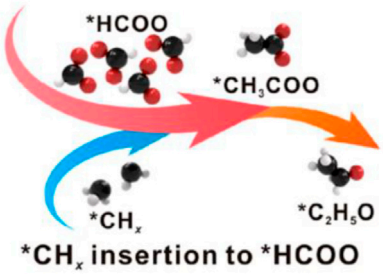

FIGURE 1
*CH_x insertion to *HCOO in C_2-oxygenates formation on the $CoAlO_x$ catalyst (Wang et al., 2019).

Catalysts

Currently, several metals have activity for the production of hydrocarbons, as shown in Table 1, among which we can mention: cobalt, iron, and bimetallic catalysts. Despite several studies employing iron-based catalysts, cobalt-based catalysts are more resistant to deactivation by water. There is a less significant effect of water on the carbon monoxide conversion rate (Khodakov et al., 2007; Díaz et al., 2014). In contrast, the presence of iron in copper catalysts can favor the catalytic activity of the hydrogenation reaction and the thermal stability of copper particles in high-temperature reactions. Furthermore, iron tends to promote the dispersion of copper, thus resulting in high surface areas.

Regarding the catalyst parameters that can influence the catalytic behavior, we can mention the particle size (Bezemer et al., 2006; Rane et al., 2012), the phase composition, the type of support and its texture (Borg et al., 2007; Cheng et al., 2015). Thus, all must be carefully controlled to obtain efficient catalysts. The main objective of any catalyst preparation for the synthesis of modified FTS is to produce a significant concentration of stable metal sites (Khodakov, 2009). For possible industrial applications, in addition to high conversions and desired product selectivity, the time for which the catalyst can keep these parameters stable is a critical factor. It is essential to note that the stability of the catalysts must also be evaluated. Some studies, such as Liu et al., Zhang et al., and Iglesias et al. (Iglesias et al., 2015; Zhang et al., 2015; Liu et al., 2018a) obtained stabilities above 100 h for iron-based catalysts with the aid of promoters.

Iron catalysts are used to synthesize hydrocarbons due to their high selectivity for the formation of primary olefins (Zhang et al., 2015). Iron-based catalysts stand out in CO_2 hydrogenation due to their activity for the RWGS and FTS reaction (Visconti et al., 2017). In CO_2 hydrogenation over Fe-based catalysts, the Fe_3O_4 phase catalyzes the RWGS reaction, and the Hägg iron carbide (χ-Fe_5C_2) phase (reduced form) provides active sites for CO hydrogenation and chain-growth (Kim et al., 2020b). Therefore, preparation methods and promoter addition have been extensively studied and impact the catalytic activity.

Cobalt catalysts have been used in industry to convert syngas into hydrocarbons and alcohols via FTS. However, due to the strong hydrogenation ability and lack of RWGS activity, the product selectivity is dominated by methane. Chakrabarti et al. (2015) explored the behavior of CO_2 on the $CoPt/Al_2O_3$ catalyst system under FTS conditions. The only products formed from CO_2 over the $CoPt/Al_2O_3$ catalyst were C_1–C_3 hydrocarbons, with methane being the dominant product. Visconti et al. (2016) also observed that, over an un-promoted Co/γ-Al_2O_3 catalyst, CO_2 is effectively hydrogenated, forming mainly methane among the products.

However, using different catalyst preparation techniques and promoters and supports, one can manage to bypass the methanation process and form other products. Selective hydrogenation of CO_2 to ethanol was reported by Wang et al. (Wang L. et al., 2018) with cobalt catalysts derived from a Co-Al layered double hydroxide (LDH), which were subjected to calcination and reduction to form alumina-supported cobalt particles ($CoAlO_x$). The catalyst reduced at 600°C showed the best catalytic performance with an ethanol selectivity of 92.1% at 140°C. The authors indicated that this improved performance is likely due to the optimized presence of surface oxide species with coexisting Co–CoO phases, which enhance the production of *CHx for converting formate into acetate by insertion, an essential intermediate for ethanol production.

Furthermore, Wang et al. (2019) indicate that methanation can be avoided by incorporating nickel into the cobalt catalyst, which would favor the formation of the stable intermediate *CHx. The *CHx intermediary is inserted into the *HCOO, which is easily formed to favor the formation of oxygenated C_2, according to Figure 1. According to the authors, the $Co_{0,52}Ni_{0,48}AlO_x$ catalyst boosts ethanol production to outperform the noble-metal-containing catalysts. The two works developed by Wang (Wang L. et al., 2018; Wang et al., 2019) expand the application of cobalt as a catalyst by shifting

methane production as the primary product and increasing the selectivity of ethanol. The works developed present different modifications of the catalysts. However, they favor the production of ethanol with the formation of $*CH_x$ species. Therefore, this is an alternative that draws attention to exploitation.

Additionally, ethanol hydrocarbons C_{5+} production can also be achieved from cobalt catalysts. There is an increase in the chemisorption of CO_2 and reduction in the adsorption of H_2, with the introduction of alkali metals. Then it suppresses the formation of CH_4 and increases the selectivity of C_{5+} at the expense of CO_2 conversion levels. Shi et al. (2018a) investigated the impact of promoting alkali metals on catalytic activity and physicochemical properties of CoCu/TiO_2 catalysts. Due to the presentation of stronger basicity and lower desorption of H_2 among the promoters used in the study, the Na-modified CoCu/TiO_2 catalyst showed the highest yield of C_{5+} (5.4% and selectivity of 42.1%) with a CO_2 conversion of 18.4%.

Tarasov et al. (2018b) evaluated the effect of the nature of the metal (Au, Pt, Fe, and Co) on the activity and selectivity of catalysts in the hydrogenation of CO_2. The authors indicate that the metals Fe and Co present activity and selectivity to C_{2+} hydrocarbons. The highest selectivity and yield of C_{5+} hydrocarbons are thus observed for 10% Co/MIL-53(Al) catalyst at 300°C and iron-containing catalyst at 400°C (= 30.8 and 4.1%, respectively). In another study, carbon dioxide conversion into liquid hydrocarbons was carried out over Co nanoparticles also embedded in the MIL-53(Al) matrix. Tarasov et al. (2018a) evaluated the 10% Co/MIL-53(Al) catalyst and observed good activity in CO_2 hydrogenation. Associated with high chemical and thermal stability, the microporous structure derived from Al_{3+} MIL-53(Al) was defined as a matrix for Co nanoparticles. The observed increase in CO_2 conversion compared to the thermodynamically possible conversion is assumed to be due to the expected shift from equilibrium to CO formation due to its rapid conversion to hydrocarbons by the Fischer-Tropsch reaction.

The CO_2 hydrogenation to liquid hydrocarbons typically occurs through RWGS reaction, followed by the hydrogenation of CO to hydrocarbons via FTS. According to He et al. (2019), Co catalyst promoted with Mn could successfully avoid the CO route. In the course of the reaction, CO_2 adsorbed on the catalyst was reduced to CH_2 monomer and CH_3 species via CO2δ−, HCOO−, $-CH_2OH$, and/or CH_3O- intermediates by H atoms. The liquid hydrocarbons were produced through chain growth steps similar to Co^0 catalyzed FTS reaction. The liquid product, C_5 to C_{26} hydrocarbons (mostly n-paraffin), could achieve selectivity of 53.2 C-mol %.

Thus, these studies show that, despite their limitations, there is ample Co-based catalysts field research in which parameters such as particle size, pretreatment, promoters, and preparation method, among others, can be explored for modified FTS.

Considering that the RWGS is a reversible reaction, the driving force for the RWGS reaction can be increased by consuming the CO intermediate to form a hydrocarbon or by decreasing the steam content in the reactor. Therefore, bimetallic catalysts are recommended since monometallic iron does not favor the increase of CO_2 conversion. Including a second metal such as cobalt has attracted much attention. The cobalt is highly active in converting CO to hydrocarbons and inactive in the WGS reaction (Geng et al., 2016), favoring high reaction rates (Satthawong et al., 2013; Gnanamani et al., 2016).

Generally, the intimacy between active sites plays a vital role in determining the catalytic performance of bifunctional catalysts. One is the Fe_3O_4 active site for RWGS, and the other is the FT active site, such as Co or iron carbide. The close contact between the Fe and Co sites favors a higher concentration of CO in the cobalt sites, which is attributed to the easy overflow of the intermediate CO from the Fe_3O_4 sites to Co and, thus, favors the production of C_{2+} hydrocarbons through the FTS reaction. Nevertheless, the distance between the Fe and Co sites leads to selectivity to methane, associated with a lower concentration of CO on the Co sites (Jiang et al., 2018).

Guo et al. (2018a) also studied the behavior of the Fe-Co bimetallic catalyst performance in the two-stage reactor system. However, considering the detrimental impact of H_2O formed by the RWGS reaction, an *ex-situ* water removal between the stages was applied, aiming at removing this product formed in the first reactor. The authors indicate that *ex-situ* water removal plays an important role in decreasing selectivity to undesired CO by-products and improving catalytic activity. Moreover, a two-stage reactor system enhanced liquid fuel yield to 300 $g_{fuels}/(kg_{cath})$ and promoted CO_2 conversion to 69,9%.

Kim et al. (2020b) synthesized, for CO_2 hydrogenation, monodisperse $CoFe_2O_4$ nanoparticles (NPs). The excellent performance of the bimetallic catalyst can be credited to the formation of bimetallic alloy carbide $(Fe1-xCox)_5C_2$, which led to better CO_2 conversion, selectivity of C_{2+} hydrocarbons and light olefins. Figure 2 shows the evolution of $CoFe_2O_4$ in the Na-$CoFe_2O_4$/CNT catalyst. $CoFe_2O_4$ was converted into a single Co-Fe alloy phase during the initial reduction of H_2 and posteriorly into the bimetallic carbide alloy $(Fe1\text{-}xCox)_5C_2$ with the Hägg carbide structure.

The hydrogenation capability of cobalt metal is higher than that of the iron catalyst; therefore, there is a benefit in the conversion of CO_2 as the cobalt charge increases. However, a higher selectivity to CH_4 is observed. This was confirmed by using the 15% Co/SiO_2 catalyst, over which CH_4 was mainly produced with a selectivity higher than 90% at different temperatures (Geng et al., 2016). Gnanamani et al. (2016) also explored the possibility of keeping iron and cobalt in proximity in a carburized form. The effect of temperature and the fraction of Fe in Co-Fe catalysts were investigated for the activity and selectivity. According to the authors, the increasing Fe fraction and the selectivity to C_2-C_4 for Co-Fe catalyst

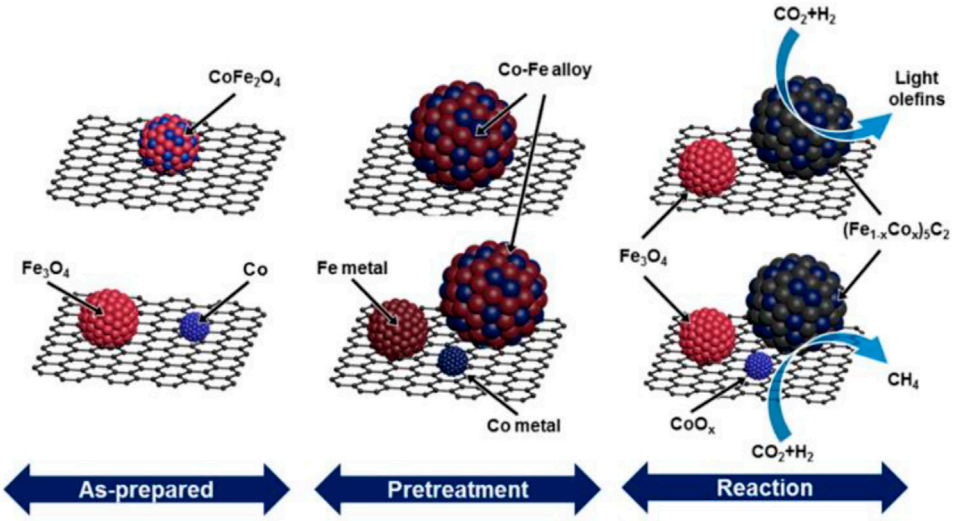

FIGURE 2
Phase transformations of as-prepared spinel $CoFe_2O_4$ NPs (top row) or (Fe_3O_4 + Co) NPs (bottom row) on CNT supports during the pre-reduction and reaction steps. (Kim et al., 2020b).

increased under all operating conditions. Among the activation conditions, the CO pretreated Co-Fe (50Co50Fe) catalyst presented a much lower methane selectivity. The bimetallic CoFe alloy is the only phase identified with the 50Co50Fe catalyst after reduction in H_2 at 350°C. The CO carburized CoFe samples contained smaller particles than those of syngas or H_2 pretreated Co–Fe models. The ^{55}Fe Mössbauer study suggests that cobalt was present in proximity to iron which is in both oxide and metallic phases. Despite this, there is the possibility of the presence of cobalt in any of the existing iron carbides. Further ongoing studies aim at establishing the structure and location of cobalt in iron carbides at lower concentrations. The CO_2 hydrogenation activity of the CO pretreated Co-Fe catalyst decreased with increasing Fe content from 0 to 50%. The 50Co50Fe catalyst exhibited fairly high selectivity toward C_2–C_4 hydrocarbons (20–25%) and oxygenates (4.0–5.0%) and a lower selectivity to methane (50–60%) in comparison to the CO-pretreated monometallic catalysts (i.e., Fe and Co). Further increases in Fe content of the catalyst did not significantly alter CO_2 hydrogenation activity and selectivity. The CO pretreated 50Co50Fe sample exhibited a low selectivity for methane (47.1%) in comparison to syngas or H_2 pretreated 50Co50Fe catalysts (69.2 and 58.5%). An even better selectivity to oxygenates (5.1 or 2.2%) and lower selectivity to methane (30.6 or 14.4%) from CO_2 was found for the 1% sodium (Na) or 1.7% potassium (K) promoted 50Co50Fe catalyst. K may be involved in the catalytic cycle for forming acetic acid, acetaldehyde, and ethanol from CO_2.

These studies show that the efficiency of Fe-Co bimetallic catalysts can be explained by improving the Fe activity Co. The cobalt has a high power to convert the intermediate CO formed in the RWGS reaction, increasing the driving force of the process and promoting hydrocarbons formation.

In contrast to other metals such as Co, Ni, and Ru, the Cu-based catalyst is well-known for not promoting CO_2 methanation (Wang et al., 2011) and for its activity in RWGS (Centi and Perathoner, 2009). In bimetallic catalysts with Cu and Fe, Cu can catalyze RWGS to produce CO, and Fe can enhance chain growth in CO hydrogenation. Thus, the work of Wang et al. (Wang W. et al., 2018) focuses on the effect of combining Fe and Cu on CO_2 hydrogenation. A series of Fe-Cu/Al_2O_3 catalysts with a wide range of Cu/(Fe + Cu) atomic ratios were prepared, and it was observed that the CO_2 conversion increases with the increasing Cu content. The maximum conversion was achieved with a ratio of 0.17, however, higher Cu ratios decreased CO_2 conversion.

Liu et al. (2018b) also studied the outcome of doping Cu into Fe-based supported catalysts. Catalysts with different Fe and Cu percentages were prepared by various impregnation methods to observe the effect of Cu on the product distribution. This effect over Fe-supported catalyst was different from that obtained using the other usual promoters (e.g., K, Mn, Zn, etc.). The selectivity of light olefins ($C_2^=$–$C_4^=$) decreased, but a significant improvement was obtained for hydrocarbons C_{5+}. The intense interaction between Cu and Fe facilitated the reduction of Fe, and CO_2 adsorption was enhanced on Cu-supported catalysts. Soon, was contributed to the improvement of CO_2 conversion, a decrease in the selectivity of CH_4, and an increase in selectivity of C_{5+}. Further, the enhanced adsorption of primarily formed olefins on Cu-promoted catalysts favored the secondary conversion of the produced olefins. Hydrogenation of olefins increased the

selectivity to paraffin, and the oligomerization of olefins increased the selectivity to C_{5+}.

Supports

In general, studies have focused on using oxides as supports. The application of various supports allows the modification of the metal dispersion, particle size, and metal-support interactions due to the physicochemical properties of the supports. Metal or non-metal oxide supports such as silica (SiO_2), alumina (Al_2O_3), titania (TiO_2) as well as carbon materials have been widely used in CO_2-FTS catalysts with alkali promoters to produce olefin-rich hydrocarbon mixtures (Hwang et al., 2020).

Owen et al. (2016) studied the effect of inorganic oxide supports (SiO_2, CeO_2, TiO_2 Al_2O_3, MgO and ZrO_2, and ZSM-5) Co-Na-Mo-based catalysts on the direct conversion of CO_2 into hydrocarbons. Catalysts supported on SiO_2 and ZSM-5 present the highest CO_2 conversion values and similar CO and hydrocarbon selectivity. The Co-Na-Mo catalysts supported on CeO_2, TiO_2, Al_2O_3, and ZrO_2 displayed a similar CO_2 conversion under the studied conditions, approximately 15%. However, the hydrocarbon selectivity/CO ratio decreases in the order of $ZrO_2 < Al_2O_3 < TiO_2 < CeO_2$. Liu et al. (2018c) also tested a series of supports, in this case, K-modified in a physical mixture with pure Fe_5C_2 catalyst. The authors observed that the alkaline Al_2O_3 favored light olefins and C_{5+} hydrocarbons production since, during the reaction, the potassium migrated into Fe_5C_2, improving the $C_{2\text{-}4}^{=}$ olefins and C_{5+} value-added hydrocarbons formation.

As seen in these two studies and among others, alumina is widely used as a support for CO_2 conversion. In this line, investigating how the surface Al–OH groups in Al_2O_3 supported catalysts can affect the FeK catalyst performance, Ding et al. (2014) conducted a study. The authors found that, in addition to favoring the CO adsorption, basic hydroxyls improve the iron particles' dispersion with a smaller particle size of iron and higher catalyst activity. Also, Piriyasurawong et al. (2021) synthesized a Fe/Ce-Al_2O_3 catalysts by one-step flame spray pyrolysis (FSP). This study observed that Ce increased the carburization process and the formation of iron carbide, improving the catalytic activity and hydrocarbon selectivity.

Kattel et al. (2016) observed that CeO_2 and ZrO_2 supported PtCo catalysts showed high CH_4 selectivity, while CO is preferentially formed with TiO_2 support. An AP-XPS analysis of model surfaces and the FTIR spectra of the powder catalysts revealed that the difference in selectivity is probably associated with different dominant reaction pathways. HCOO/*HOCO and $*CH_3O$ were observed on PtCo/CeO_2 and PtCo/ZrO_2 as reaction intermediates, while *HCOO/*HOCO was observed on PtCo/TiO_2 catalyst.

In addition to these parameters, the pore size distribution of supports is also significant in determining the catalytic performance and product distribution. It can profoundly impact the dispersion of metals, reducibility, and mass transport performance. In this line, the increasing catalyst pore sizes lead to the higher olefins/paraffins ratios due to the enhancement of product diffusion, alleviating the hydrogenation of re-adsorbed olefins to paraffins. A too-small pore size distribution is unfavorable for the reaction as it leads to a minimum particle size that is not adequate for C–C bond growth (Xie C. et al., 2017; Numpilai et al., 2019).

To provide insights into the role of the metal-support interaction on the CO_2 hydrogenation system, Torrente-Murciano et al. (2016), synthesized a series of nanostructured ceria materials. The study demonstrates that the morphology of the ceria support on Fe/CeO_2 catalyst plays a vital role in CO_2 conversion, methane to hydrocarbon selectivity, and olefin to paraffin ratio. The modification of the iron reactivity is related to the high metal-support interaction shown by the shift of the reduction temperatures of the Fe/CeO_2 catalysts concerning their corresponding supports, associated with the selective exposure of different crystal planes in the different ceria morphologies.

Carbon-based supports are an excellent alternative to oxides. Carbon nanotubes, carbon spheres, vitreous carbons, and activated carbon have a good surface area; their pore structures can be adjusted, thus favoring a lower interaction with the active metallic catalyst due to its inert characteristic. Hwang et al. (2020) fabricated well-defined mesoporous carbon (MPC) and used it as a support material for Fe catalysts to produce liquid fuels. The MPC support promoted the formation of Fe_7C_3, which is an active phase for FTS, due to weak metal-support interaction. The mesoporous structure provided the benefits of fast mass transfer of hydrocarbon molecules, which enhanced CO_2 conversion and C_{5+} hydrocarbon selectivity.

Regarding iron nanoparticles supported on oxygen- and nitrogen-functionalized multi-walled carbon nanotubes (OCNTs and NCNTs) and SiO_2, Chew et al. (2014b) observed that the iron oxide nanoparticles have a lower reduction rate on SiO_2 than on CNTs support. This behavior can be explained by the strong metal–support (Fe/SiO_2) interactions that make it challenging to reduce Fe and consequently interfere with the catalytic activity. Between OCNTs and NCNTs, the NCNTs promotes the iron oxide nanoparticles reduction at lower temperatures and produce the highest olefin selectivity ($C_{2\text{-}5}^{=}$).

Wang et al. (Wang S. et al., 2020) also evaluated carbon materials. The authors fabricated iron–potassium catalysts supported by single- and multi-walled carbon nanotubes, FeK/SWNTs, and FeK/MWNTs. The study finds that the FeK/MWNTs catalyst favors the selectivity of $C_{2\text{-}4}$ olefins (30.7%), whereas the FeK/SWNTs catalyst favors the selectivity of C_{5+} olefins (39.8%). Besides high productivity of heavy olefins, the FeK/SWNTs catalyst also provides much lower selectivities to

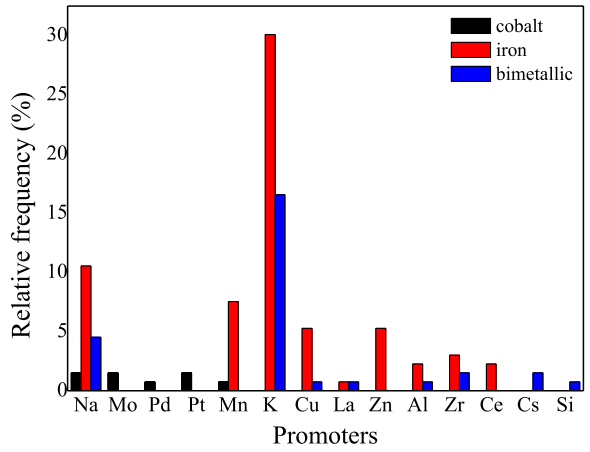

FIGURE 3
Frequency of application of promoters in Co, Fe, and bimetallic catalysts.

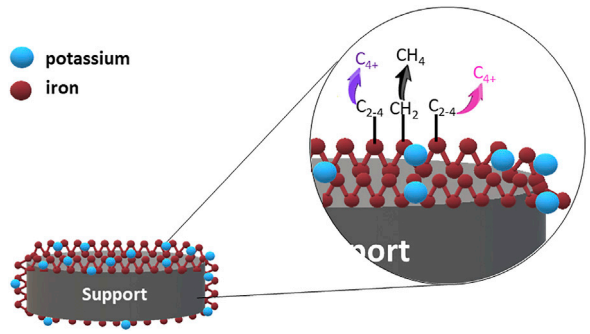

FIGURE 4
Scheme of favoring C_{2+} selectivity with the addition of promoters.

unwanted CO and CH_4. Its excellent catalytic performance is tentatively explained by the high inclination of SWNTs with large curvature to donate electrons that facilitate the dissociation of the C–O bond. It incites the formation of carbon monomers and ameliorates the carbon/hydrogen surface ratio, helpful to the formation of olefins.

Dong et al. (2020) explored the phase change, particle size, and CO_2 hydrogenation performance of a Na-promoted Fe and Co catalyst derived from ZIF-67. According to the authors, there was an excellent selectivity to olefins associated with the formation of the NC layer, which anchored and dispersed the nanoparticles, promoting the reduction and carburization of the metal. However, the pyrolysis temperature influences the degree of carbonization of the support, metallic charge, and particle size. For temperatures above 500°C, ZIF-67 is fully pyrolyzed, and the nanoparticles are well incorporated into the generated carbon support.

Promoters

The alkali metals, principally Na and K, are the most efficacious promoters (Figure 3), limiting methane formation and improving selectivity to C_{2+} products (Figure 4). According to Table 2, there has been an increase in studies using bimetallic catalysts in recent years, mainly using promoters such as K and Na. When evaluating the selectivity to CH_4, there is an average reduction for Co and Fe catalysts of 23 and 42%, respectively. For bimetallic catalysts, such as CoFe (without the addition of promoters), selectivity ranges for CH_4 and C_2-C_4 are at 45 and 20%, respectively. On the other hand, with the addition of K and Na, there is a reduction in CH_4 and C_2-C_4 paraffinic selectivity. However, the formation of C_2-C4 olefins is favored. Regarding C_{5+} selectivity, the addition of promoters is more pronounced in Fe catalysts when compared to Co and bimetallic catalysts, with an average increase above 100%.

K favors CO and CO_2 adsorption, increases the chain growth probability, inhibits secondary reactions, and enhances olefins production. Also, it can stabilize the texture of Fe-Al-O spinel, increase the surface Fe_5C_2 content and strengthen CO_2 adsorption (Iglesias et al., 2015). Ramirez et al. (2018) studied the promotion of the resulting Fe (41 wt%)-carbon composites with Cu, Mo, Li, Na, K, Mg, Ca, Zn, Ni, Co, Mn, Fe, Pt, and Rh), and observed that only K can increase the olefins selectivity. Thus, iron oxide and iron carbides favor the absorption of CO_2 and CO while reducing the affinity of H_2, increasing the selectivity to olefins. However, its effects on the product selectivity and the catalyst activity are strongly dependent on its concentration and the reaction conditions, including the nature of the reacting mixture containing CO or CO_2 (Visconti et al., 2017).

Given this, Satthawong et al. (2015) explored the effect of K on FeCo-catalyzed CO_2 hydrogenation. The authors found that the addition of potassium enhanced the activity and stability of iron carbide for the hydrogenation of carbon dioxide. Still, the hydrogenation function of the catalyst is suppressed with increasing K levels in the catalyst, resulting in higher selectivity for CO and oxygenates. The authors proposed a model for the hydrogen absorption states on catalysts with and without K. The selectivity to oxygenates increases (to a maximum of 18 C %, CO free) with the increasing K content. Besides, the potassium shifts the product distribution of C_2 oxygenates from CO_2 towards acetic acid. So, with the addition of potassium, the weakly adsorbed hydrogen on the catalyst surface suppresses the hydrogenation of the produced olefins, resulting in the high olefin content in the hydrocarbon product. Moreover, at the same reaction condition, Fe–Co(0.17)/K (1.0)/Al_2O_3 catalyst also showed higher CO_2 conversion and higher yield of light olefins than the K-promoted Fe–Ce and Fe-Mn/Al_2O_3 which are known as promising catalysts for hydrocarbon production from CO_2 hydrogenation.

TABLE 2 Main catalysts and promoters used in modified FTS.

	Catalyst Conditions					Selectivity (%)					Reaction Conditions			Ref
Metal	Promoter	Support	Pore (nm)	Particle Size (nm)	X_{CO2}	CO	CH_4	C_2-C_4	C_2-$C_4^=$	C_{5+}	H_2/CO_2	T (°C)	P (MPa)	
Co	Na, Mo	SiO_2	5,000		43.9	6.9	45.5	31.3	12.8	10.4	3/1	370	0.1	Owen et al. (2013b)
	Pd	Al_2O_3	1.9		33.0		94.7	4.8		0.5	3/1	220	2.0	Chakrabarti et al. (2015)
	Na	SiO_2	20		16.0		80.0	19			3/1	220	1.9	Gnanamani et al. (2015)
	Na, Mo	SiO_2			30.0	21.5	57.1	30.4	0.1	12.3	3/1	200	0.1	Owen et al. (2016)
	Pt	$mSiO_2$, CeO_2			3.0	75.0	60.0	40.0			3/1	250	0.6	Xie T. et al. (2017)
	Pt	Co_3O_4	26.5		27.8		60.0	25.2	14.8		3/1	200	2.0	Ouyang et al. (2017)
	Mn				15.3	0.4		46.6		53.4	1/1	200	8.0	He et al. (2019)
	Na	Ac	0.6	6.2	67.2	0.1	96.0	3.6		0.4	3/1	250	5.0	Zhang S. et al. (2020)
Fe	K	ZrO_2			43.0	15.0	18.0	9.2	44.0	28.8	3/1	340	2.0	Wang et al. (2013)
	K			20–50	38.0	7.3	21.0	14.0	34.0	30	3/1	340	2.0	You et al. (2013)
	K	Al_2O_3	7.9		54.4	14.0	26.7	10.3	26.7	36.2	3/1	400	3.0	Ding et al. (2014)
	K				29.0	8.0	63.0	31.0		6.0	3/1	330	1.0	Iglesias et al. (2015)
	K				41.0	2.0	27.2	50.3		22.5	5/1	300	1.1	Fischer et al. (2016)
	K	Al_2O_3		5–8	42.5	23.9	30.0	40.5		29.6[f]	3/1	400	3.0	Xie T. et al. (2017)
	K		6		45.0	13.0	18.4	5.7	41.4	34.5	3/1	300	0.5	Visconti et al. (2017)
	K		6.5		72.0	1.0	13.5	33.7		52.8	3/1	320	2.0	Landau et al. (2017)
	K	K/a-Al_2O_3			44.8	23.2	30.1	6.3	29.8	33.9	3/1	400	3.0	Liu et al. (2018c)
	K	HSG	14.9				25.0	12.0	59.0	4.0	3/1	340	2.0	Wu et al. (2018)
	K	C			40.0	21.0	16.5	11.4	46.8[d]	25.3[g]	3/1	350	3.0	Ramirez et al. (2018)
	K	K_2CO_3			44.0	13.0	16.1	9.2	72.4[e]	2.3	3/1	350	3.0	Ramirez et al. (2019a)
	K	MPC	8.1	15	50.6	8.2	16.8	34.7		48.5	3/1	300	2.5	Hwang et al. (2020)
	K	SWNTs		4.6	52.7	9.6	13.5	8.6	22.5	55.4	3/1	340	2.0	Wang S. et al. (2020)
	K	C			24.0	40.0	25.0	41.7		33.3	2/1	350	2.0	Pokusaeva et al. (2020)
	K				41.9	8.9	22.7	8.3	42.7	26.4	3/1	320	3.0	Liu et al. (2021b)
	K	C-1EDA		7.4	20.1	31.7	17.2	5.6	37.7	39.5	3/1	300	1.0	Kosol et al. (2021)
	K, Cu	SiO_2			27.0	35.0	12.0	33.0		55.0	3/1	250	2.0	Gnanamani et al. (2013)
	K, Cu, La	TiO_2			27.0	32.0	10.3	30.9		58.8	3/1	300	1.0	Rodemerck et al. (2013)
	K, Mn	Al_2O_3			33.4	11.0	26.4	52.4		21.1	3/1	300	1.8	Drab et al. (2013)
	K, Mn	Al_2O_3			60.0	13.4	25.9	74.1			3/1	300	1.8	Willauer et al. (2013)
	K, Cu, Al		4.3		77.0	2.0	14.6	6.7	30.3	48.3	4/1	300	1.0	Landau et al. (2014)
	Mn		19.1		30.0	7.7	29.3	63.2		3.9[g]	3/1	340	2.0	Al-Dossary et al. (2015)
	K, Zn		27.7		51.0	6.0	34.9	7.8	53.6	3.7	3/1	320	0.5	Zhang et al. (2015)
	K, Cu, Al				51.0	16.0	79.8	20.2			3/1	325	15	Mokou et al. (2015)
	Na	CNT			24.0		21.0	7.0	45	27.0	3/1	370	0.8	Mattia et al. (2015)
	K, HZSM-5		26.8		43.9	6.1	10.1	11.5		78.4	3/1	300	2.5	Geng et al. (2016)
	K, Zn, Cu		9		8.90	19.5						220	3.0	Visconti et al. (2016)
	Na		16.7		40.5	13.5	15.8	7.5	46.6	30.1	3/1	320	3.0	Wei et al. (2016)
	Na, HZSM-5			13.1	34.0	13.0	9.0	24.0		67.0	3/1	320	3.0	Wei et al. (2017)
	K, Mn	Macrolite®			36.0	8.4	27.2	72.8			3/1	320	2.0	Bradley et al. (2017a)
	K, Mn	NCNT			30.1	72.1	23.0	57.8		19.1	3/1	360	2.5	Kangvansura et al. (2017)
	K, Zn, Cu		11.6		15.1	23.4	13.2	25.5		61.4	2/1	230	1.6	Ning et al. (2014)
	K, Cu	Al_2O_3			41.0	5.7	6.8	93.2			3/1	300	2.0	Bradley et al. (2017b)
	K, Zr			25	45.0	7.0	14.0	37.2			3/1	320	2.0	Samanta et al. (2017)
	Zn, Na			2,500	34.0	11.7	9.7	31.8		58.5	3/1	340	1.0	Choi et al. (2017b)
	biopromoters	C		6–8	31.0	23.2	11.8	63.9	33.2	50.3	3/1	320	1.0	Guo et al. (2018b)
	Ni	Al_2O_3-HZSM-5			81.7	9.3	20.5	0.3		79.2	3/1	300	1.0	Bashiri et al. (2018)
	Ru	BMI-NTf2 IL			12.0		2.0	57.0		41.0	4/1	150	0.9	Qadir et al. (2018)
	K, Zn	NC		6	34.6	21.2	24.2	7.1	40.6	28.0	3/1	320	3.0	Liu et al. (2018a)
	K, Zr, Ce		2.43	21.2	54.3	3.1	20.6	7.9	55.6	15.9	3/1	320	2.0	Zhang et al. (2018)
	Rb				27.3		27.8	66.3		5.9	3/1	270	1.2	Gnanamani et al. (2018)
	K, Mg	Al_2O_3			33.5	24.9	68.1	27.8		4.1	27/10	400	3.0	Tarasov et al. (2018b)
	Na, Mn				27.9	24.1	13.1	5.3	33.9	47.6	3/1	320	0.5	Liu B. et al. (2018)
	Ni			8.4	94.1	0.7	78.2	19.7		2.1	5/1	300	0.3	Puga and Corma, (2018)

(Continued on following page)

TABLE 2 (*Continued*) Main catalysts and promoters used in modified FTS.

	Catalyst Conditions					Selectivity (%)					Reaction Conditions			Ref
Metal	Promoter	Support	Pore (nm)	Particle Size (nm)	X_{CO2}	CO	CH_4	C_2-C_4	C_2-$C_4^=$	C_{5+}	H_2/CO_2	T (°C)	P (MPa)	
	K, ZSM-5				48.4	13.9	18.1		15.3	27.1	3/1	375	3.0	Ramirez et al. (2019b)
	Na		16.8	52.1	36.8	6.0	7.7	12.8	68.4		3/1	320	3.0	Liang et al. (2019a)
	Na, Mn	Fe_3O_4		49.1	38.6	11.7	13.4	4.5	34.3		3/1	320	3.0	Liang et al. (2019b)
	Na, Zn, HZSM-5				41.2	7.0	2.0	12.0	2.0	84.0	3/1	320	3.0	Cui et al. (2019)
	Na, HZSM-5				29.4	23.1	15.1	26,3	1.4	57.2	3/1	320	1.0	Xu et al. (2019)
	Zn				34.6	17.1	26.9	23.2	29.4	20.4	56/25	300	1.0	Guo et al. (2020)
	Na, Mn		9.8	14.5	31.8	25.1	39.1	7.8	38.7	14.4	3/1	290	1.5	Zhang Z. et al. (2020)
	Na			20.7	35.3	13.2	31.8	10[c]	57.0[c]	1.2	3/1	290	1.5	Wei et al. (2020)
	Na, HZSM-5	C			33.3	13.3	4.8	9.6	0.8	84.8	3/1	320	3.0	Wang Y. et al. (2020)
	Mn		36.8		44.7	9.4	22.0	7.1	46.2	24.7	3/1	350	2.0	Jiang et al. (2020)
	K, Al				48.0	16.0	12.7	6.3	65.8	15.2[g]	4/1	300	1.0	Elishav et al. (2020)
	Pd	Graphite Oxide			21.4		49.7	21.0	21.4	7.9[h]	3/1	370	0.1	Owen et al. (2020)
	K, ZSM-5	C			34.5	20.0	11.0	16.0	3.0	70.0	5/2	320	2.0	Guo et al. (2021)
	K, Mn, Ti		24	28.2	44.9	9.6	14.1	33.9		51.9	14/5	360	5.0	Zhao et al. (2021)
	Na				41.0	15.5	14.1	3.2	30.9	51.8	3/1	330	1.5	Liu X. et al., 2021
	Zn, Zr, HZSM-5		16.6		18.0	24.0	2.0	41.0		57.0	3/1	340	5.0	Wang et al. (2021)
	K, ZSM-5				53.0	15.1	19.0	33.0[i]	9.0	39.0	3/1	375	3.0	Ramirez et al. (2021)
	K, Zn, Al		26.1		38.6		8.0	18.0		74.0	3/1	300	2.5	Nasriddinov et al. (2022)
	Na, Zn			12	39.0	14.0	12.0	4.7	43.0	40.5	3/1	340	2.5	Zhang et al. (2022a)
	Na, Ce			14.5	39.7	8.0	43.7	10.7[b]	43,3[b]	2.2[g]	3/1	320	2.0	Zhang et al. (2022b)
	Ce, Zr		8.9		26.6	77.8	62.6	28.4[j]	9[j]		3/1	370	0.1	Lino et al. (2022)
Fe-Co	K	Al_2O_3			31.0	18.0	15.9	84.1			3/1	300	1.1	Satthawong et al. (2013)
	K	Al_2O_3	22		31.0	18.0	15.9	5.5	27.4	51.2		300	1.1	Satthawong et al. (2015)
	Na		43.8		22.7	42.1	66.5	31.7		1.7	5/2	270	0.9	Gnanamani et al. (2016)
	K	Al_2O_3	45.7		37.6	24.5	13.8	4.3	33.0	24.4	3/1	320	2.0	Numpilai et al. (2017)
	K				14.2	26.2	36.5	32.6			3/1	240	1.2	Gnanamani et al. (2017)
	K, Zr				43.0			53.0	30.0		3/1	400	3.0	Li et al. (2018)
	K				54.6	2.0	19.3	7.9	24.9	48.0	3/1	300	2.5	Jiang et al. (2018)
	K				69.9	3.2	16.7	31.8		51.5	17/50	330	3.0	Guo et al. (2018a)
	K, Zr		11.6		58.0	59.0	11.0	14.0	62.0	8.0	4/1	310	2.0	Ding et al. (2019)
	K	K-Al_2O_3			41.6	12.1	32.2	6.0	41.2	20.6	3/1	320	2.0	Numpilai et al. (2019)
	Na	CNT		10–20	33.7	18.0	15.6	7.7	38.2	38.5	3/1	340	1.0	Kim et al. (2020b)
	K	Al_2O_3			41.0	10.0	27.0	9.5	44.5	19.0	3/1	340	2.0	Numpilai et al. (2020)
	K	Al_2O_3			40.0	12.2	24.8	7.9	46.1	21.2	3/1	340	2.0	Chaipraditgul et al. (2021)
	Zn			8.3	49.6	5.8	19.0	6.0	36.1	38.9	3/1	320	2.5	Xu et al. (2021)
	Na				41.8	9.7	22.1	7.6	41.2	29.0	3/1	320	3.0	Yuan et al. (2021)
	Na	Al_2O_3			32.8	8.1	13.7	4.9	32.5	48.9	1/1	350	3.0	Dai et al. (2021)
	K, La	Al_2O_3	9.67		24.0	10.0			100		3/1	300	1.0	Bashiri et al. (2021)
	Cu, Al, K, Na		3.2		52.9	2.3	8.2	40.9	32.9	18.0	3/1	300	2.0	Zheng et al. (2021)
Fe-Cu	K	Al_2O_3	18		31.5		29.0	71.0[c]			3/1	300	1.1	Satthawong et al. (2014)
	Cs				39.0	6.3		68,7		31.3	3/1	350	5.0	Ando, (2016)
	K	Al_2O_3	20		29.3	17.0	8.4	91,6			3/1	300	1.1	Wang W. et al. (2018)
	K			14	26.2	36.2	13.5	54.1		32.4	3/1	290	1.7	Pour et al. (2018)
	K	Al_2O_3	4.96		41.7	26.5	37.8	41.2	2.2	18.8	3/1	400	3.0	Liu et al. (2018b)
	K, La	TiO_2	31.7		23.2	33.0	19.4	37.3		43.3	3/1	300	1.1	Boreriboon et al. (2018)
	Cs, Si		7.8		16.0		33.0	59.0		8	3/1	270	1.3	Shafer et al. (2019)
	K, Al		33	33.5	37.0	10.8	9.1	31.8		59.1	3/1	300	2.5	Hwang et al. (2019)
	K, SAPO-34				49.7	16.0	10.7	10.7	75.0	3.6	4/1	340	1.5	Ding et al. (2021)
Co-Cu	K	TiO_2	30.9		13.0	35.1	34.1	30.8		35.1	3/1	250	5.0	Shi et al. (2018b)
	Na	TiO_2	24.1		18.4	30.2	26.1	31.8		42.1	3/1	250	5.0	Shi et al. (2018a)
Fe-Cr	K	Nb_2O_5			20.0	33.0	53.7	9.0	37.3		3/1	400	0.1	da Silva and Mota, (2019)

= : olefinic products; b: C5-C6; c: C2-C7; d: C2-C6; e: C2-C10; f: C5-C7; g: C7+; h: C4+; i: C2-C9; j: C2-C3.

The critical parameter to be observed is the different loading levels of K in the iron-based CO_2 hydrogenation. Higher K loadings increased the chain growth probability. Further, the K promotion directly enhances the formation of χ-Fe_5C_2 under reaction conditions but, at higher concentrations, has a detrimental impact on the FT activity without directly influencing the RWGS reaction (Fischer et al., 2016). There is an improvement in CO_2 hydrogenation to light olefins over Fe-based catalyst by changing the content of the K promotor and, hence, setting the bonding strengths of adsorbed species. The K/Fe atomic ratio of 2.5 exhibited the maximum C_{2-4} olefins distribution (46.7%) and O/P ratio of 7.6. This is because the K increases the bonding strength of adsorbed CO_2 and H_2 species, reducing the hydrogenation of olefins to paraffins. However, the catalyst that obtained the highest yield of light olefins (16.4%) was with 0.5 KFe catalyst. This is justified by the K enriched surface in K/Fe of 2.5, drastically reducing the surface area and creating a hydrogen-lean environment, ultimately diminishing catalytic activity (Numpilai et al., 2020). Visconti et al. (2017) have found that careful control of the calcination process allows achieving high surface area and avoids transforming the spinel structure (Fe_3O_4/γ-Fe_2O_3) into the more stable corundum structure of γ-Fe_2O_3. The authors prepared a high surface area K-promoted iron-based catalyst. The catalyst was synthetized The catalyst was synthetized by thermal decomposition of ammonium glycolate complexes and then by impregnating an aqueous solution of K carbonate, drying, and calcination. The prepared catalyst performs better than two reference model samples (K-α-Fe_2O_3 and K-Fe_3O_4) in CO_2 hydrogenation. In turn, this results in a better catalytic activity because of the maximization of type II sites (active in CO activation and C–C bond formation) compared to type I sites (involved in the WGS/RWGS process).

Geng et al. (2016) aimed at suppressing the formation of CO and CH_4, thus investigated K-promoted supported and unsupported iron catalysts and different reaction conditions, reactor systems, and zeolites for the catalytic conversion of CO_2. The iron supported on different supports by K-promotion displayed undesirably high selectivities to CO ranging from 23.2 to 54.5% and selectivities to CH_4 ranging from 22.4 to 41.2% at similar conversions of approximately 40%. In contrast, the precipitated iron 92.6Fe7.4K catalyst showed significantly higher activity (41.7%), very low selectivity to CO (6%) and CH_4 (10.3%), and high olefins (C_2–C_4) selectivity (77.7%) under the same reaction conditions. The low selectivity to CO might be ascribed to a larger active iron carbide surface, which increases the chances of CO-FTS. In addition, to produce gasoline-range isoparaffins, the catalyst 92.6Fe7.4K was mixed with 0.5 Pd or HZSM-5 zeolite. The HZSM-5 showed a higher isoparaffin selectivity (70%) due to hydrocracking and hydroisomerization of FT olefin primary products. Figure 5 shows the reaction path of CO_2 hydrogenation through iron catalyst and zeolite.

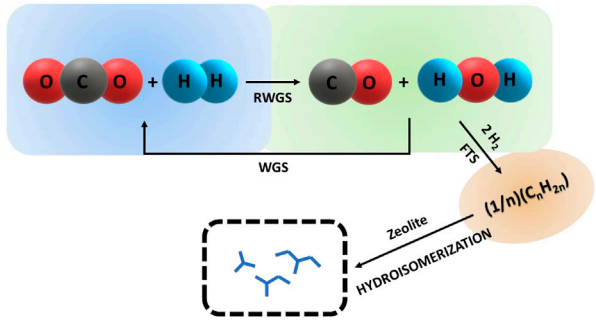

FIGURE 5
Reaction network for isoparaffin synthesis by CO_2-based FTS followed by hydroisomerization of the FT products (Geng et al., 2016).

K is the most used promoter, as shown in Table 2. However, studies simultaneously use K and lanthanum (La) promoters. The combination of La and K can adjust the H and C coverage on the catalyst surface, which is essential in changing product distribution in CO_2 hydrogenation. Boreriboon et al. (2018) reported the outcomes of K and La promoting in Fe–Cu/TiO_2 catalyst on hydrocarbon production from CO_2 hydrogenation. The promoted catalyst gave higher C_{5+} hydrocarbons selectivity (29 C-mol%) than the unpromoted catalyst (21 C-mol%). And the characterization showed that the K addition could significantly reduce the amount of chemisorbed H_2 species and increase chemisorbed CO_2 species on the catalyst surface. Furthermore, La addition is able to promote the moderately adsorbed CO_2 species (principally monodentate carbonate species), which leads to increasing C_5–C_7 selectivity.

In addition to K and La, Na has also been proposed to enhance both the activity and the selectivity to heavy hydrocarbons and olefins in FT synthesis (da Silva and Mota, 2019). Na was frequently introduced to catalysts employing a precipitating agent on the account that it is difficult to thoroughly remove the residual Na during washing of the precipitates (Huang et al., 2010). Therefore, it is crucial to discuss this effect on the catalyst's physico-chemical properties and catalytic performance. Based on this, Wei et al. (2016) prepared a series of Fe_3O_4-based nanocatalysts with different residual Na contents. The FeNa (1.18) catalyst exhibited the maximum olefin/paraffin ratio and the largest total C_2–C_4 olefins and C_{5+} yield with a higher CO_2 conversion among the FeNa(x) series. The authors observed that increasing the residual Na promotes the surface basicity and dramatically improves the carburization degrees of the iron catalysts. Likewise, Liang et al. (2019a) also indicated that adding the Na promoter favors the increase of CO_2 adsorption, the formation and stability of Fe_2C_2, and inhibits the secondary hydrogenation of alkenes. By increasing the amount of Na, both CO_2 conversion and selectivity to alkenes are favored, the highest being 36.8 and

64.3%, respectively, while the corresponding methane production decreases to 7.2%. *In situ* Raman spectra and temperature-programmed profiles performed by Wei et al. (2020) indicated that the presence of the Na promoter also favors carbon deposits by CO dissociation and inhibits surface carbon reduction by H_2. As a result, the intermediate carbon species hydrogenation is limited, favoring enhanced of olefins.

Manganese (Mn) was also the subject of studies for Fe-based catalysts to favor the high selectivity of light olefins. Thus, Liu et al. (Liu B. et al., 2018) investigated the effects of promoting Na and Mn in Fe_3O_4-based catalysts in CO_2 hydrogenation to produce light α-olefins. The authors observed that both Mn and Na promoters can increase the reducibility of Fe_3O_4. However, the promotional mechanism for Na and Mn in the reduction behavior is different. The authors proposed a mechanism for the promotional reducibility of iron oxides by the presence of oxygen vacancies in MnO and by the donation of electrons from Na. In this case, Na favors the reduction by electron donation to Fe as the oxygen vacancy formation energy is expressively diminished in the presence of Na. In contrast, the oxygen vacancy in MgO promotes reduction as the oxygen in Fe oxide can spontaneously overflow into the vacancy in MnO. In addition, Jiang et al. (2020) synthesized Mn well-dispersed on Fe_3O_4 microsphere (Mn–Fe_3O_4) catalyst and investigated the mechanism of the Mn-modulation effect on the C=O band activation and C–C chain growth. The study indicated that adding Mn to Fe-based catalysts could facilitate the C=O bond activation in the RWGS reaction of CO_2 hydrogenation and inhibit C–C chain growth and the hydrogenation improving the selectivity and yield of olefins.

In opposition, the results obtained by Zhang et al. (Zhang Z. et al., 2020) show that the selectivity of light olefins decreases from 38.73 to 30.58%. In comparison, the ratio olefin/paraffin decreases from 4.97 to 3.56, with the content of Mn promoters in FeNa catalyst increasing from 0.5 to 10.0%. With the increasing content of the Mn, the strong adsorption of CO_2 is confirmed on surface Fe species near the Mn promoters, which possibly decreases the conversion of CO_2. Furthermore, the increasing content of Mn increases the adsorption ability of H_2 on the surface of iron carbides, which is associated with the secondary hydrogenation of intermediates to paraffins and consequently decreases the ratio of olefins to paraffins. The electronic effect of Mn promoters on the nature of Fe-based active species and the catalytic consequences during CO_2 hydrogenation is a very controversial topic. The same debate is open to the electronic effects of zinc during CO and CO_2 hydrogenation processes. With the scope of identifying the most influential promoter, Falbo et al. (2017) studied the outcomes of Zn or Mn association in the structure of a Fe-based catalyst. The authors found that the two catalysts have resemblant textural and morphological properties, with elevated surface areas, a predominance of the crystalline Fe_2O_3 phase, and the presence of $ZnFe_2O_4$ and $MnFe_2O_4$. However, different from Mn, the stronger CO_2 adsorptions keep the H/C ratio on the surface low in the Zn-promoted sample. As a result, the products shift toward long-chain and unsaturated hydrocarbons. Likewise, Zhang et al. (2015) prepared a series of K-promoted Fe–Zn catalysts with varied Fe/Zn molar ratios and applied them to CO_2 hydrogenation reaction via FTS for the selective production of C_2–C_4 olefins. Results showed that the addition of zinc to the iron matrix formed the $ZnFe_2O_4$ spinel phase and ZnO phase, caused an increase in the surface areas, enhanced the interaction between iron and zinc, and altered the reduction and CO_2 adsorption behaviors. In contrast to the results obtained by Falbo et al. (2017), the appropriate interactions between Fe and Zn demonstrate to be advantageous in repressing the C_{5+} hydrocarbons production and promoting the production of light olefins. The 1Fe–1Zn–K catalyst with H_2/CO reduction exhibited a higher performance with the CO_2 conversion of 51%. The selectivity of C_2–C_4 olefins in overall hydrocarbons and the olefin ratio to paraffin in the C_2–C_4 fraction reached 53.5 and 6.8%, respectively. Therefore, Zn serves as a structural promoter to suppress the growth of Fe particles. In contrast, Na serves as an electronic promoter to modify the catalytic activity and selectivity of the Fe particles. The combination of Zn and Na with Fe increases the CO_2 adsorption properties. It promotes the *in situ* formation of Hägg iron carbide (χ-Fe_5C_2), the active phase for forming heavy hydrocarbons in CO_2 hydrogenation (Choi et al., 2017b).

Although iron-based catalysts are a feasible route to olefins production from CO_2, one challenge is their vulnerability to water produced during the reaction. An additional route to increasing a catalyst's resistance to water is to add elements that are more resistant to oxidation. to get around this effects of water on iron-based catalysts, Bradley et al. (2017b) added copper (10–30%) to the catalyst blend to improve catalyst activity and durability. The authors showed that adding 10% copper decreases the selectivity of CH_4 and CO and considerably increases the CO_2 conversion. Moreover, copper does not influence the catalyst's crystallinity or dispersion but generates some phase separation effects if the quantity of copper is too high. According to the authors, the FeCu/K catalyst creates an inverse spinel crystal phase, independent of the amount of metal. Furthermore, the formation of this phase is favored with the loading of Cu (>10%).

Conclusion

The use of CO_2 and H_2 as clean hydrocarbons sources remains a challenge, gaining emphasis in the last years due to the potential for reducing CO_2 emissions and introducing renewable energy in the chemical industry and automotive market.

Several routes have been evaluated for hydrogenating CO_2 into hydrocarbons. This review summarizes the FTS pathway

catalytic hydrogenation progress of CO_2, which consists of a modified FT reaction, where CO_2 reacts instead of CO.

The reaction occurs in two steps. Firstly, CO_2 reacts with H_2 in the RWGS to form CO, and then CO reacts in the traditional FT reactions to form hydrocarbons. The reaction coupling of RWGS and carbon chain growth should proceed synergistically to achieve high selectivity towards the desired heavy hydrocarbons instead of a more undesirable CO product. Therefore, the reaction requires a catalyst that has to be active in both the RWGS and the FT reactions. Because of their higher activity in RWGS, Fe-based catalysts are preferred (usually doped with alkali metals) over Co-based catalysts.

This review shows that alkali metals, especially K, are essential as promoters for obtaining high selectivity to olefins. K is an excellent promoter increasing the catalyst carburization process and decreasing H_2 adsorption. As a result, a higher activity in the chain growth process and an inhibition of the secondary hydrogenation of olefins is obtained. Following potassium, Na has been the most used promoter because it favors the formation and stability of Fe_2C_2, increases the CO_2 conversion by improving surface adsorption, and inhibits the hydrogenation, enhancing olefins selectivity.

The most common support used in modified FTS is γ-Al_2O_3. Their modification with K and Ce enhanced light olefins and C_{5+} hydrocarbons formation and increased the carburization process and the formation of iron carbide, respectively. SiO_2 supports difficult iron oxide nanoparticle reduction by strongly interacting with the metal and the support. Carbon-based supports have a lower interaction with the active metallic catalyst due to their inert characteristic. Nontraditional supports, such as MOFs and porous carbons, need further research to increase stability and lower olefin yields.

Many technological and economic impediments still have to be overcome. Economically feasible technical and catalytic advances are still required for the large-scale conversion of CO_2 to value-added hydrocarbons. However, economic and social incentives can encourage investigations that aim at developing more efficient catalysts.

Author contributions

JA, PR, and ES-A contributed to conception and design of the study. MT and GW organized the database. MT wrote the first draft of the manuscript. GW, JA, PR, and ES-A wrote sections of the manuscript. All authors contributed to manuscript revision, read, and approved the submitted version.

Conflict of interest

The authors declare that the research was conducted in the absence of any commercial or financial relationships that could be construed as a potential conflict of interest.

Publisher's note

References

Al-Dossary, M., Ismail, A. A., Fierro, J. L. G., Bouzid, H., and Al-Sayari, S. A. (2015). Effect of Mn loading onto MnFeO nanocomposites for the CO_2 hydrogenation reaction. *Appl. Catal. B Environ.* 165, 651–660. doi:10.1016/j.apcatb.2014.10.064

Albrecht, M., Rodemerck, U., Schneider, M., Bröring, M., Baabe, D., and Kondratenko, E. V. (2017). Unexpectedly efficient CO_2 hydrogenation to higher hydrocarbons over non-doped Fe2O3. *Appl. Catal. B Environ.* 204, 119–126. doi:10.1016/j.apcatb.2016.11.017

Ando, H. (2016). Selective alkene production by the hydrogenation of carbon dioxide over Fe-Cu catalyst. *Energy Procedia* 89, 421–427. doi:10.1016/j.egypro.2016.05.056

Bashiri, N., Omidkhah, M. R., and Godini, H. R. (2021). Direct conversion of CO_2 to light olefins over FeCo/XK-ϒAL2O3 (X = La, Mn, Zn) catalyst via hydrogenation reaction. *Res. Chem. Intermed.* 47 (12), 5267–5289. doi:10.1007/s11164-021-04562-z

Bashiri, N., Royaee, S. J., and Sohrabi, M. (2018). The catalytic performance of different promoted iron catalysts on combined supports Al2O3 for carbon dioxide hydrogenation. *Res. Chem. Intermed.* 44 (1), 217–229. doi:10.1007/s11164-017-3099-9

Bezemer, G. L., Bitter, J. H., Kuipers, H. P. C. E., Oosterbeek, H., Holewijn, J. E., Xu, X., et al. (2006). Cobalt particle size effects in the Fischer-Tropsch reaction studied with carbon nanofiber supported catalysts. *J. Am. Chem. Soc.* 128 (12), 3956–3964. doi:10.1021/ja058282w

Boreriboon, N., Jiang, X., Song, C., and Prasassarakich, P. (2018). Higher hydrocarbons synthesis from CO_2 hydrogenation over K- and La-promoted Fe–Cu/TiO2 catalysts. *Top. Catal.* 61 (15–17), 1551–1562. doi:10.1007/s11244-018-1023-1

Borg, O., Eri, S., Blekkan, E. A., Storsaeter, S., Wigum, H., Rytter, E., et al. (2007). Fischer-Tropsch Synthesis over alpha-alumina-supported cobalt catalysts: Effect of support variables. *J. Catal.* 248 (1), 89–100. doi:10.1016/j.jcat.2007.03.008

Bradley, M. J., Ananth, R., Willauer, H. D., Baldwin, J. W., Hardy, D. R., DiMascio, F., et al. (2017a). The role of catalyst environment on CO_2 hydrogenation in a fixed-bed reactor. *J. CO2 Util.* 17, 1–9. doi:10.1016/j.jcou.2016.10.014

Bradley, M. J., Ananth, R., Willauer, H. D., Baldwin, J. W., Hardy, D. R., and Williams, F. W. (2017b). The effect of copper addition on the activity and stability of iron-based CO_2 hydrogenation catalysts. *Molecules* 22 (9), 1579. doi:10.3390/molecules22091579

Centi, G., and Perathoner, S. (2009). Opportunities and prospects in the chemical recycling of carbon dioxide to fuels. *Catal. Today* 148 (3–4), 191–205. doi:10.1016/j.cattod.2009.07.075

Chaipraditgul, N., Numpilai, T., Kui Cheng, C., Siri-Nguan, N., Sornchamni, T., Wattanakit, C., et al. (2021). Tuning interaction of surface-adsorbed species over Fe/K-Al2O3 modified with transition metals (Cu, Mn, V, Zn or Co) on light olefins production from CO_2 hydrogenation. *Fuel* 283, 119248. doi:10.1016/j.fuel.2020.119248

Chakrabarti, D., De Klerk, A., Prasad, V., Gnanamani, M. K., Shafer, W. D., Jacobs, G., et al. (2015). Conversion of CO_2 over a co-based Fischer-Tropsch catalyst. *Ind. Eng. Chem. Res.* 54 (4), 1189–1196. doi:10.1021/ie503496m

Chen, T., Jiang, W., Sun, X., Ning, W., Liu, Y., Xu, G., et al. (2020). Size-controlled synthesis of hematite α-Fe2O3 nanodisks closed with (0001) basal facets and {11-20} side facets and their catalytic performance for CO_2 hydrogenation. *ChemistrySelect* 5 (1), 430–437. doi:10.1002/slct.201904490

Chen, Y., Choi, S., and Thompson, L. T. (2016). Low temperature CO_2 hydrogenation to alcohols and hydrocarbons over Mo2C supported metal catalysts. *J. Catal.* 343, 147–156. doi:10.1016/j.jcat.2016.01.016

Cheng, K., Virginie, M., Ordomsky, V. V., Cordier, C., Chernavskii, P. A., Ivantsov, M. I., et al. (2015). Pore size effects in high-temperature Fischer–Tropsch Synthesis over supported iron catalysts. *J. Catal.* 328, 139–150. doi:10.1016/j.jcat.2014.12.007

Chernyak, S. A., Ivanov, A. S., Stolbov, D. N., Maksimov, S. V., Maslakov, K. I., Chernavskii, P. A., et al. (2020). Sintered Fe/CNT framework catalysts for CO_2 hydrogenation into hydrocarbons. *Carbon N. Y.* 168, 475–484. doi:10.1016/j.carbon.2020.06.067

Chew, L. M., Kangvansura, P., Ruland, H., Schulte, H. J., Somsen, C., Xia, W., et al. (2014b). Effect of nitrogen doping on the reducibility, activity and selectivity of carbon nanotube-supported iron catalysts applied in CO_2 hydrogenation. *Appl. Catal. A General* 482, 163–170. doi:10.1016/j.apcata.2014.05.037

Chew, L. M., Ruland, H., Schulte, H. J., Xia, W., and Muhler, M. (2014a). CO_2 hydrogenation to hydrocarbons over iron nanoparticles supported on oxygen-functionalized carbon nanotubes. *J. Chem. Sci.* 126 (2), 481–486. doi:10.1007/s12039-014-0591-2

Choi, Y. H., Jang, Y. J., Park, H., Kim, W. Y., Lee, Y. H., Choi, S. H., et al. (2017a). Carbon dioxide fischer-tropsch synthesis: A new path to carbon-neutral fuels. *Appl. Catal. B Environ.* 202, 605–610. doi:10.1016/j.apcatb.2016.09.072

Choi, Y. H., Ra, E. C., Kim, E. H., Kim, K. Y., Jang, Y. J., Kang, K. N., et al. (2017b). Sodium-containing spinel zinc ferrite as a catalyst precursor for the selective synthesis of liquid hydrocarbon fuels. *ChemSusChem* 10 (23), 4764–4770. doi:10.1002/cssc.201701437

Cui, X., Gao, P., Li, S., Yang, C., Liu, Z., Wang, H., et al. (2019). Selective production of aromatics directly from carbon dioxide hydrogenation. *ACS Catal.* 9 (5), 3866–3876. doi:10.1021/acscatal.9b00640

Cui, Y., Guo, L., Gao, W., Wang, K., Zhao, H., He, Y., et al. (2021). From single metal to bimetallic sites: Enhanced higher hydrocarbons yield of CO_2 hydrogenation over bimetallic catalysts. *ChemistrySelect* 6 (21), 5241–5247. doi:10.1002/slct.202101072

da Silva, I. A., and Mota, C. J. A. (2019). Conversion of CO_2 to light olefins over iron-based catalysts supported on niobium oxide. *Front. Energy Res.* 7, 1–8. doi:10.3389/fenrg.2019.00049

Dai, C., Zhao, X., Hu, B., Zhang, X., Luo, Q., Guo, X., et al. (2021). Effect of EDTA-2Na modification on Fe-Co/Al2O3for hydrogenation of carbon dioxide to lower olefins and gasoline. *J. CO2 Util.* 43, 101369. doi:10.1016/j.jcou.2020.101369

Das, T., and Deo, G. (2012a). Effects of metal loading and support for supported cobalt catalyst. *Catal. Today* 198 (1), 116–124. doi:10.1016/j.cattod.2012.04.028

Das, T., and Deo, G. (2012b). Promotion of alumina supported cobalt catalysts by iron. *J. Phys. Chem. C* 116 (39), 20812–20819. doi:10.1021/jp3007206

Díaz, J. A., Calvo-Serrano, M., De La Osa, A. R., García-Minguillán, A. M., Romero, A., Giroir-Fendler, A., et al. (2014). β-Silicon carbide as a catalyst support in the Fischer-Tropsch Synthesis: Influence of the modification of the support by a pore agent and acidic treatment. *Appl. Catal. A General* 475, 82–89. doi:10.1016/j.apcata.2014.01.021

Ding, F., Zhang, A., Liu, M., Zuo, Y., Li, K., Guo, X., et al. (2014). CO_2 hydrogenation to hydrocarbons over iron-based catalyst: Effects of physicochemical properties of Al2O3 supports. *Ind. Eng. Chem. Res.* 53 (45), 17563–17569. doi:10.1021/ie5031166

Ding, J., Huang, L., Gong, W., Fan, M., Zhong, Q., Russell, A. G., et al. (2019). CO_2 hydrogenation to light olefins with high-performance Fe0.30Co0.15Zr0.45K0.10O1.63. *J. Catal.* 377, 224–232. doi:10.1016/j.jcat.2019.07.036

Ding, J., Liu, Q., Ye, R. P., Gong, W., Zhang, F., He, X., et al. (2021). Metal-support interactions in Fe-Cu-K admixed with SAPO-34 catalysts for highly selective transformation of CO_2 and H_2 into lower olefins. *J. Mat. Chem. A Mat.* 9 (38), 21877–21887. doi:10.1039/d1ta03327a

Dong, Z., Zhao, J., Tian, Y., Zhang, B., and Wu, Y. (2020). Preparation and performances of ZIF-67-derived FeCo bimetallic catalysts for CO_2 hydrogenation to light olefins. *Catalysts* 10 (4), 455. doi:10.3390/catal10040455

Drab, D. M., Willauer, H. D., Olsen, M. T., Ananth, R., Mushrush, G. W., Baldwin, J. W., et al. (2013). Hydrocarbon synthesis from carbon dioxide and hydrogen: A two-step process. *Energy fuels.* 27 (11), 6348–6354. doi:10.1021/ef4011115

Elishav, O., Shener, Y., Beilin, V., Landau, M. V., Herskowitz, M., Shter, G. E., et al. (2020). Electrospun Fe-Al-O nanobelts for selective CO_2 hydrogenation to light olefins. *ACS Appl. Mat. Interfaces* 12 (22), 24855–24867. doi:10.1021/acsami.0c05765

Falbo, L., Martinelli, M., Visconti, C. G., Lietti, L., Forzatti, P., Bassano, C., et al. (2017). Effects of Zn and Mn promotion in Fe-based catalysts used for CO_x hydrogenation to long-chain hydrocarbons. *Ind. Eng. Chem. Res.* 56 (45), 13146–13156. doi:10.1021/acs.iecr.7b01494

Fischer, N., Henkel, R., Hettel, B., Iglesias, M., Schaub, G., and Claeys, M. (2016). Hydrocarbons via CO_2 hydrogenation over iron catalysts: The effect of potassium on structure and performance. *Catal. Lett.* 146 (2), 509–517. doi:10.1007/s10562-015-1670-9

Gao, P., Li, S., Bu, X., Dang, S., Liu, Z., Wang, H., et al. (2017). Direct conversion of CO_2 into liquid fuels with high selectivity over a bifunctional catalyst. *Nat. Chem.* 9 (10), 1019–1024. doi:10.1038/nchem.2794

Garbarino, G., Cavattoni, T., Riani, P., and Busca, G. (2020). Support effects in metal catalysis: A study of the behavior of unsupported and silica-supported cobalt catalysts in the hydrogenation of CO_2 at atmospheric pressure. *Catal. Today* 345, 213–219. doi:10.1016/j.cattod.2019.10.016

Geng, S., Jiang, F., Xu, Y., and Liu, X. (2016). Iron-based fischer-tropsch synthesis for the efficient conversion of carbon dioxide into isoparaffins. *ChemCatChem* 8 (7), 1303–1307. doi:10.1002/cctc.201600058

Gnanamani, M. K., Hamdeh, H. H., Jacobs, G., Shafer, W. D., Hopps, S. D., Thomas, G. A., et al. (2017). Hydrogenation of carbon dioxide over K-promoted FeCo bimetallic catalysts prepared from mixed metal oxalates. *ChemCatChem* 9 (7), 1303–1312. doi:10.1002/cctc.201601337

Gnanamani, M. K., Hamdeh, H. H., Shafer, W. D., Hopps, S. D., and Davis, B. H. (2018). Hydrogenation of carbon dioxide over iron carbide prepared from alkali metal promoted iron oxalate. *Appl. Catal. A General* 564, 243–249. doi:10.1016/j.apcata.2018.07.034

Gnanamani, M. K., Jacobs, G., Hamdeh, H. H., Shafer, W. D., and Davis, B. H. (2013). Fischer-Tropsch synthesis: Mössbauer investigation of iron containing catalysts for hydrogenation of carbon dioxide. *Catal. Today* 207, 50–56. doi:10.1016/j.cattod.2012.02.059

Gnanamani, M. K., Jacobs, G., Hamdeh, H. H., Shafer, W. D., Liu, F., Hopps, S. D., et al. (2016). Hydrogenation of carbon dioxide over Co-Fe bimetallic catalysts. *ACS Catal.* 6 (2), 913–927. doi:10.1021/acscatal.5b01346

Gnanamani, M. K., Jacobs, G., Keogh, R. A., Shafer, W. D., Sparks, D. E., Hopps, S. D., et al. (2015). Fischer-Tropsch synthesis: Effect of pretreatment conditions of cobalt on activity and selectivity for hydrogenation of carbon dioxide. *Appl. Catal. A General* 499, 39–46. doi:10.1016/j.apcata.2015.03.046

Guo, L., Cui, Y., Zhang, P., Peng, X., Yoneyama, Y., Yang, G., et al. (2018a). Enhanced liquid fuel production from CO_2 hydrogenation: Catalytic performance of bimetallic catalysts over a two-stage reactor system. *ChemistrySelect* 3 (48), 13705–13711. doi:10.1002/slct.201803335

Guo, L., Li, J., Zeng, Y., Kosol, R., Cui, Y., Kodama, N., et al. (2020). Heteroatom doped iron-based catalysts prepared by urea self-combustion method for efficient CO_2 hydrogenation. *Fuel* 276, 118102. doi:10.1016/j.fuel.2020.118102

Guo, L., Sun, J., Ji, X., Wei, J., Wen, Z., Yao, R., et al. (2018b). Directly converting carbon dioxide to linear α-olefins on bio-promoted catalysts. *Commun. Chem.* 1 (1), 11–18. doi:10.1038/s42004-018-0012-4

Guo, L., Sun, S., Li, J., Gao, W., Zhao, H., Zhang, B., et al. (2021). Boosting liquid hydrocarbons selectivity from CO_2 hydrogenation by facilely tailoring surface acid properties of zeolite via a modified Fischer-Tropsch synthesis. *Fuel* 306, 121684. doi:10.1016/j.fuel.2021.121684

Guo, L., Zhang, P., Cui, Y., Liu, G., Wu, J., Yang, G., et al. (2019). One-pot hydrothermal synthesis of nitrogen functionalized carbonaceous material catalysts with embedded iron nanoparticles for CO_2 hydrogenation. *ACS Sustain. Chem. Eng.* 7 (9), 8331–8339. doi:10.1021/acssuschemeng.8b06795

Gupta, S., Jain, V. K., and Jagadeesan, D. (2016). Fine tuning the composition and nanostructure of Fe-based core–shell nanocatalyst for efficient CO_2 hydrogenation. *ChemNanoMat* 2 (10), 989–996. doi:10.1002/cnma.201600234

He, Z., Cui, M., Qian, Q., Zhang, J., Liu, H., and Han, B. (2019). Synthesis of liquid fuel via direct hydrogenation of CO_2. *Proc. Natl. Acad. Sci. U. S. A.* 116 (26), 12654–12659. doi:10.1073/pnas.1821231116

Huang, L., Qin, Z., Wang, G., Du, M., Ge, H., Li, X., et al. (2010). A detailed study on the negative effect of residual sodium on the performance of Ni/ZnO adsorbent for diesel fuel desulfurization. *Ind. Eng. Chem. Res.* 49 (10), 4670–4675. doi:10.1021/ie100293h

Hwang, S. M., Han, S. J., Min, J. E., Park, H. G., Jun, K. W., and Kim, S. K. (2019). Mechanistic insights into Cu and K promoted Fe-catalyzed production of liquid hydrocarbons via CO_2 hydrogenation. *J. CO2 Util.* 34, 522–532. doi:10.1016/j.jcou.2019.08.004

Hwang, S. M., Zhang, C., Han, S. J., Park, H. G., Kim, Y. T., Yang, S., et al. (2020). Mesoporous carbon as an effective support for Fe catalyst for CO_2 hydrogenation to liquid hydrocarbons. *J. CO2 Util.* 37, 65–73. doi:10.1016/j.jcou.2019.11.025

Iglesias, G. M., De Vries, C., Claeys, M., and Schaub, G. (2015). Chemical energy storage in gaseous hydrocarbons via iron Fischer-Tropsch synthesis from H_2/CO_2 - kinetics, selectivity and process considerations. *Catal. Today* 242, 184–192. doi:10.1016/j.cattod.2014.05.020

Jiang, F., Liu, B., Geng, S., Xu, Y., and Liu, X. (2018). Hydrogenation of CO_2 into hydrocarbons: Enhanced catalytic activity over Fe-based Fischer-Tropsch catalysts. *Catal. Sci. Technol.* 8 (16), 4097–4107. doi:10.1039/c8cy00850g

Jiang, J., Wen, C., Tian, Z., Wang, Y., Zhai, Y., Chen, L., et al. (2020). Manganese-promoted Fe3O4 microsphere for efficient conversion of CO_2 to light olefins. *Ind. Eng. Chem. Res.* 59 (5), 2155–2162. doi:10.1021/acs.iecr.9b05342

Jimenez, J. D., Wen, C., and Lauterbach, J. (2019). Design of highly active cobalt catalysts for CO_2 hydrogenation: Via the tailoring of surface orientation of nanostructures. *Catal. Sci. Technol.* 9 (8), 1970–1978. doi:10.1039/c9cy00402e

Jimenez, J. D., Wen, C., Royko, M. M., Kropf, A. J., Segre, C., and Lauterbach, J. (2020). Influence of coordination environment of anchored single-site cobalt catalyst on CO_2 hydrogenation. *ChemCatChem* 12 (3), 846–854. doi:10.1002/cctc.201901676

Kangvansura, P., Chew, L. M., Kongmark, C., Santawaja, P., Ruland, H., Xia, W., et al. (2017). Effects of potassium and manganese promoters on nitrogen-doped carbon nanotube-supported iron catalysts for CO_2 hydrogenation. *Engineering* 3 (3), 385–392. doi:10.1016/J.ENG.2017.03.013

Kattel, S., Yu, W., Yang, X., Yan, B., Huang, Y., Wan, W., et al. (2016). CO_2 hydrogenation over oxide-supported PtCo catalysts: The role of the oxide support in determining the product selectivity. *Angew. Chem. Int. Ed. Engl.* 55 (28), 8100–8105. doi:10.1002/ange.201601661

Khodakov, A. Y., Chu, W., and Fongarland, P. (2007). Advances in the development of novel cobalt Fischer – Tropsch catalysts for synthesis of long-chain hydrocarbons and clean fuels. *Chem. Rev.* 107 (5), 1692–1744. doi:10.1021/cr050972v

Khodakov, A. Y. (2009). Fischer-Tropsch Synthesis: Relations between structure of cobalt catalysts and their catalytic performance. *Catal. Today* 144 (3–4), 251–257. doi:10.1016/j.cattod.2008.10.036

Kim, K. Y., Lee, H., Noh, W. Y., Shin, J., Han, S. J., Kim, S. K., et al. (2020b). Cobalt ferrite nanoparticles to form a catalytic Co-Fe alloy carbide phase for selective CO_2 hydrogenation to light olefins. *ACS Catal.* 10 (15), 8660–8671. doi:10.1021/acscatal.0c01417

Kim, Y., Kwon, S., Song, Y., and Na, K. (2020a). Catalytic CO_2 hydrogenation using mesoporous bimetallic spinel oxides as active heterogeneous base catalysts with long lifetime. *J. CO2 Util.* 36, 145–152. doi:10.1016/j.jcou.2019.11.005

Kosol, R., Guo, L., Kodama, N., Zhang, P., Reubroycharoen, P., Vitidsant, T., et al. (2021). Iron catalysts supported on nitrogen functionalized carbon for improved CO_2 hydrogenation performance. *Catal. Commun.* 149, 106216. doi:10.1016/j.catcom.2020.106216

Landau, M. V., Meiri, N., Utsis, N., Vidruk Nehemya, R., and Herskowitz, M. (2017). Conversion of CO_2, CO, and H_2 in CO_2 hydrogenation to fungible liquid fuels on Fe-based catalysts. *Ind. Eng. Chem. Res.* 56 (45), 13334–13355. doi:10.1021/acs.iecr.7b01817

Landau, M. V., Vidruk, R., and Herskowitz, M. (2014). Sustainable production of green feed from carbon dioxide and hydrogen. *ChemSusChem* 7 (3), 785–794. doi:10.1002/cssc.201301181

Li, W., Zhang, A., Jiang, X., Janik, M. J., Qiu, J., Liu, Z., et al. (2018). The anti-sintering catalysts: Fe–Co–Zr polymetallic fibers for CO_2 hydrogenation to C2 = –C4 = –rich hydrocarbons. *J. CO2 Util.* 23, 219–225. doi:10.1016/j.jcou.2017.07.005

Li, Z., Liu, J., Shi, R., Waterhouse, G. I. N., Wen, X. D., and Zhang, T. (2021). Fe-based catalysts for the direct photohydrogenation of CO_2 to value-added hydrocarbons. *Adv. Energy Mat.* 11 (12), 2002783–2002789. doi:10.1002/aenm.202002783

Liang, B., Duan, H., Sun, T., Ma, J., Liu, X., Xu, J., et al. (2019a). Effect of Na promoter on Fe-based catalyst for CO_2 hydrogenation to alkenes. *ACS Sustain. Chem. Eng.* 7 (1), 925–932. doi:10.1021/acssuschemeng.8b04538

Liang, B., Sun, T., Ma, J., Duan, H., Li, L., Yang, X., et al. (2019b). Mn decorated Na/Fe catalysts for CO_2 hydrogenation to light olefins. *Catal. Sci. Technol.* 9 (2), 456–464. doi:10.1039/c8cy02275e

Lino, A. V. P., Assaf, E. M., and Assaf, J. M. (2022). Production of light hydrocarbons at atmospheric pressure from CO_2 hydrogenation using CexZr(1-x)O2 iron-based catalysts. *J. CO2 Util.* 55 (2021), 101805. doi:10.1016/j.jcou.2021.101805

Liu, B., Geng, S., Zheng, J., Jia, X., Jiang, F., and Liu, X. (2018). Unravelling the new roles of Na and Mn promoter in CO_2 hydrogenation over Fe3O4-based catalysts for enhanced selectivity to light α-olefins. *ChemCatChem* 10 (20), 4718–4732. doi:10.1002/cctc.201800782

Liu, J., Li, K., Song, Y., Song, C., and Guo, X. (2021a). Selective hydrogenation of $CO_2$to hydrocarbons: Effects of Fe3O4Particle size on reduction, carburization, and catalytic performance. *Energy fuels.* 35 (13), 10703–10709. doi:10.1021/acs.energyfuels.1c01265

Liu, J., Sun, Y., Jiang, X., Zhang, A., Song, C., and Guo, X. (2018a). Pyrolyzing ZIF-8 to N-doped porous carbon facilitated by iron and potassium for CO_2 hydrogenation to value-added hydrocarbons. *J. CO2 Util.* 25, 120–127. doi:10.1016/j.jcou.2018.03.015

Liu, J., Zhang, A., Jiang, X., Liu, M., Sun, Y., Song, C., et al. (2018b). Selective CO_2 hydrogenation to hydrocarbons on Cu-promoted Fe-based catalysts: Dependence on Cu-Fe interaction. *ACS Sustain. Chem. Eng.* 6 (8), 10182–10190. doi:10.1021/acssuschemeng.8b01491

Liu, J., Zhang, A., Jiang, X., Liu, M., Zhu, J., Song, C., et al. (2018c). Direct transformation of carbon dioxide to value-added hydrocarbons by physical mixtures of Fe5C2 and K-modified Al2O3. *Ind. Eng. Chem. Res.* 57 (28), 9120–9126. doi:10.1021/acs.iecr.8b02017

Liu, J., Zhang, A., Jiang, X., Zhang, G., Sun, Y., Liu, M., et al. (2019). Overcoating the surface of Fe-based catalyst with ZnO and nitrogen-doped carbon toward high selectivity of light olefins in CO_2 hydrogenation. *Ind. Eng. Chem. Res.* 58 (10), 4017–4023. doi:10.1021/acs.iecr.8b05478

Liu, J., Zhang, A., Liu, M., Hu, S., Ding, F., Song, C., et al. (2017). Fe-MOF-derived highly active catalysts for carbon dioxide hydrogenation to valuable hydrocarbons. *J. CO2 Util.* 21, 100–107. doi:10.1016/j.jcou.2017.06.011

Liu, J., Zhang, G., Jiang, X., Wang, J., Song, C., and Guo, X. (2021b). Insight into the role of Fe5C2 in CO_2 catalytic hydrogenation to hydrocarbons. *Catal. Today* 371, 162–170. doi:10.1016/j.cattod.2020.07.032

Liu, X., Zhang, C., Tian, P., Xu, M., Cao, C., Yang, Z., et al. (2021). Revealing the effect of sodium on iron-based catalysts for CO_2 hydrogenation: Insights from calculation and experiment. *J. Phys. Chem. C* 125 (14), 7637–7646. doi:10.1021/acs.jpcc.0c11123

Martinelli, M., Visconti, C. G., Lietti, L., Forzatti, P., Bassano, C., and Deiana, P. (2014). CO_2 reactivity on Fe-Zn-Cu-K Fischer-Tropsch synthesis catalysts with different K-loadings. *Catal. Today* 228, 77–88. doi:10.1016/j.cattod.2013.11.018

Mattia, D., Jones, M. D., O'Byrne, J. P., Griffiths, O. G., Owen, R. E., Sackville, E., et al. (2015). Towards carbon-neutral CO_2 conversion to hydrocarbons. *ChemSusChem* 8 (23), 4064–4072. doi:10.1002/cssc.201500739

Minett, D. R., O'Byrne, J. P., Pascu, S. I., Plucinski, P. K., Owen, R. E., Jones, M. D., et al. (2014). Fe@CNT-monoliths for the conversion of carbon dioxide to hydrocarbons: Structural characterisation and Fischer-Tropsch reactivity investigations. *Catal. Sci. Technol.* 4 (9), 3351–3358. doi:10.1039/c4cy00616j

Mokou, C., Beisswenger, L., Vogel, H., Klemenz, S., and Albert, B. (2015). "Iron-catalyzed hydrogenation of carbon dioxide to hydrocarbons/fuels in condensed phase," in 2015 5th International Youth Conference on Energy (IYCE), (Pisa, Italy: IEEE), 1–6.

Nasriddinov, K., Min, J-E., Park, H-G., Han, S. J., Chen, J., Jun, K-W., et al. (2022). Effect of Co, Cu, and Zn on FeAlK catalysts in CO_2 hydrogenation to C 5+ hydrocarbons. *Catal. Sci. Technol.* 12 (3), 906–915. doi:10.1039/d1cy01980e

Ning, W., Wang, T., Chen, H., Yang, X., and Jin, Y. (2014). The effect of Fe_2O_3 crystal phases on CO_2 hydrogenation. *Acta Crystallogr. Sect. A Found. Adv.* 70 (1), C49. doi:10.1371/journal.pone.0182955

Numpilai, T., Chanlek, N., Poo-Arporn, Y., Cheng, C. K., Siri-Nguan, N., Sornchamni, T., et al. (2020). Tuning interactions of surface-adsorbed species over Fe–Co/K–Al2O3 catalyst by different K contents: Selective CO_2 hydrogenation to light olefins. *ChemCatChem* 12 (12), 3306–3320. doi:10.1002/cctc.202000347

Numpilai, T., Chanlek, N., Poo-Arporn, Y., Wannapaiboon, S., Cheng, C. K., Siri-Nguan, N., et al. (2019). Pore size effects on physicochemical properties of Fe-Co/K-Al 2 O 3 catalysts and their catalytic activity in CO_2 hydrogenation to light olefins. *Appl. Surf. Sci.* 483, 581–592. doi:10.1016/j.apsusc.2019.03.331

Numpilai, T., Witoon, T., Chanlek, N., Limphirat, W., Bonura, G., Chareonpanich, M., et al. (2017). Structure–activity relationships of Fe-Co/K-Al2O3 catalysts calcined at different temperatures for CO_2 hydrogenation to light olefins. *Appl. Catal. A General* 547, 219–229. doi:10.1016/j.apcata.2017.09.006

Ouyang, B., Xiong, S., Zhang, Y., Liu, B., and Li, J. (2017). The study of morphology effect of Pt/Co3O4 catalysts for higher alcohol synthesis from CO_2 hydrogenation. *Appl. Catal. A General* 543, 189–195. doi:10.1016/j.apcata.2017.06.031

Owen, R. E., Cortezon-Tamarit, F., Calatayud, D. G., Evans, E. A., Mitchell, S. I. J., Mao, B., et al. (2020). Shedding light onto the nature of iron decorated graphene and graphite oxide nanohybrids for CO_2 conversion at atmospheric pressure. *ChemistryOpen* 9 (2), 242–252. doi:10.1002/open.201900368

Owen, R. E., O'Byrne, J. P., Mattia, D., Plucinski, P., Pascu, S. I., and Jones, M. D. (2013b). Cobalt catalysts for the conversion of CO_2 to light hydrocarbons at atmospheric pressure. *Chem. Commun.* 49 (99), 11683–11685. doi:10.1039/c3cc46791k

Owen, R. E., O'Byrne, J. P., Mattia, D., Plucinski, P., Pascu, S. I., and Jones, M. D. (2013a). Promoter effects on iron-silica fischer-tropsch nanocatalysts: Conversion of carbon dioxide to lower olefins and hydrocarbons at atmospheric pressure. *Chempluschem* 78 (12), 1536–1544. doi:10.1002/cplu.201300263

Owen, R. E., Plucinski, P., Mattia, D., Torrente-Murciano, L., Ting, V. P., and Jones, M. D. (2016). Effect of support of Co-Na-Mo catalysts on the direct conversion of CO_2 to hydrocarbons. *J. CO2 Util.* 16, 97–103. doi:10.1016/j.jcou.2016.06.009

Piriyasurawong, K., Panpranot, J., Mekasuwandumrong, O., and Praserthdam, P. (2021). CO_2 hydrogenation over FSP-made iron supported on cerium modified alumina catalyst. *Catal. Today* 375, 307–313. doi:10.1016/j.cattod.2020.03.007

Pokusaeva, Y. A., Koklin, A. E., Eliseev, O. L., Kazantsev, R. V., and Bogdan, V. I. (2020). Hydrogenation of carbon oxides over the Fe-based catalysts on the carbon support. *Russ. Chem. Bull.* 69 (2), 237–240. doi:10.1007/s11172-020-2751-5

Pour, A. N., Housaindokht, M. R., and Asil, A. G. (2018). Production of higher hydrocarbons from CO_2 over nanosized iron catalysts. *Chem. Eng. Technol.* 41 (3), 479–488. doi:10.1002/ceat.201700490

Puga, A. V., and Corma, A. (2018). Hydrogenation of CO_2 on nickel–iron nanoparticles under sunlight irradiation. *Top. Catal.* 61 (18–19), 1810–1819. doi:10.1007/s11244-018-1030-2

Qadir, M. I., Bernardi, F., Scholten, J. D., Baptista, D. L., and Dupont, J. (2019). Synergistic CO_2 hydrogenation over bimetallic Ru/Ni nanoparticles in ionic liquids. *Appl. Catal. B Environ.* 252, 10–17. doi:10.1016/j.apcatb.2019.04.005

Qadir, M. I., Weilhard, A., Fernandes, J. A., De Pedro, I., Vieira, B. J. C., Waerenborgh, J. C., et al. (2018). Selective carbon dioxide hydrogenation driven by ferromagnetic RuFe nanoparticles in ionic liquids. *ACS Catal.* 8 (2), 1621–1627. doi:10.1021/acscatal.7b03804

Ramirez, A., Dutta Chowdhury, A., Dokania, A., Cnudde, P., Caglayan, M., Yarulina, I., et al. (2019b). Effect of zeolite topology and reactor configuration on the direct conversion of CO_2 to light olefins and aromatics. *ACS Catal.* 9 (7), 6320–6334. doi:10.1021/acscatal.9b01466

Ramirez, A., Gevers, L., Bavykina, A., Ould-Chikh, S., and Gascon, J. (2018). Metal organic framework-derived iron catalysts for the direct hydrogenation of CO_2 to short chain olefins. *ACS Catal.* 8 (10), 9174–9182. doi:10.1021/acscatal.8b02892

Ramirez, A., Gong, X., Caglayan, M., Nastase, S. A. F., Abou-Hamad, E., Gevers, L., et al. (2021). Selectivity descriptors for the direct hydrogenation of CO_2 to hydrocarbons during zeolite-mediated bifunctional catalysis. *Nat. Commun.* 12 (1), 5914. doi:10.1038/s41467-021-26090-5

Ramirez, A., Ould-Chikh, S., Gevers, L., Chowdhury, A. D., Abou-Hamad, E., Aguilar-Tapia, A., et al. (2019a). Tandem conversion of CO_2 to valuable hydrocarbons in highly concentrated potassium iron catalysts. *ChemCatChem* 11 (12), 2879–2886. doi:10.1002/cctc.201900762

Rane, S., Borg, O., Rytter, E., and Holmen, A. (2012). Relation between hydrocarbon selectivity and cobalt particle size for alumina supported cobalt Fischer-Tropsch catalysts. *Appl. Catal. A General* 437–438, 10–17. doi:10.1016/j.apcata.2012.06.005

Rodemerck, U., Holeňa, M., Wagner, E., Smejkal, Q., Barkschat, A., and Baerns, M. (2013). Catalyst development for CO_2 hydrogenation to fuels. *ChemCatChem* 5 (7), 1948–1955. doi:10.1002/cctc.201200879

Samanta, A., Landau, M. V., Vidruk-Nehemya, R., and Herskowitz, M. (2017). CO_2 hydrogenation to higher hydrocarbons on K/Fe-Al-O spinel catalysts promoted with Si, Ti, Zr, Hf, Mn and Ce. *Catal. Sci. Technol.* 7 (18), 4048–4063. doi:10.1039/c7cy01118k

Satthawong, R., Koizumi, N., Song, C., and Prasassarakich, P. (2013). Bimetallic Fe-Co catalysts for CO_2 hydrogenation to higher hydrocarbons. *J. CO2 Util.* 3–4, 102–106. doi:10.1016/j.jcou.2013.10.002

Satthawong, R., Koizumi, N., Song, C., and Prasassarakich, P. (2014). Comparative study on CO_2 hydrogenation to higher hydrocarbons over Fe-based bimetallic catalysts. *Top. Catal.* 57 (6–9), 588–594. doi:10.1007/s11244-013-0215-y

Satthawong, R., Koizumi, N., Song, C., and Prasassarakich, P. (2015). Light olefin synthesis from CO_2 hydrogenation over K-promoted Fe-Co bimetallic catalysts. *Catal. Today* 251, 34–40. doi:10.1016/j.cattod.2015.01.011

Sedighi, M., and Mohammadi, M. (2020). CO_2 hydrogenation to light olefins over Cu-CeO2/SAPO-34 catalysts: Product distribution and optimization. *J. CO2 Util.* 35, 236–244. doi:10.1016/j.jcou.2019.10.002

Shafer, W. D., Jacobs, G., Graham, U. M., Hamdeh, H. H., and Davis, B. H. (2019). Increased CO_2 hydrogenation to liquid products using promoted iron catalysts. *J. Catal.* 369, 239–248. doi:10.1016/j.jcat.2018.11.001

Shi, Z., Yang, H., Gao, P., Chen, X., Liu, H., Zhong, L., et al. (2018a). Effect of alkali metals on the performance of CoCu/TiO2 catalysts for CO_2 hydrogenation to long-chain hydrocar-bons. *Chin. J. Catal.* 39 (8), 1294–1302. doi:10.1016/S1872-2067(18)63086-4

Shi, Z., Yang, H., Gao, P., Li, X., Zhong, L., Wang, H., et al. (2018b). Direct conversion of CO_2 to long-chain hydrocarbon fuels over K-promoted CoCu/TiO2 catalysts. *Catal. Today* 311, 65–73. doi:10.1016/j.cattod.2017.09.053

Skrypnik, A. S., Yang, Q., Matvienko, A. A., Bychkov, V. Y., Tulenin, Y. P., Lund, H., et al. (2021). Understanding reaction-induced restructuring of well-defined FexOyCz compositions and its effect on CO_2 hydrogenation. *Appl. Catal. B Environ.* 291, 120121. doi:10.1016/j.apcatb.2021.120121

Srisawad, N., Chaitree, W., Mekasuwandumrong, O., Shotipruk, A., Jongsomjit, B., and Panpranot, J. (2012). CO_2 hydrogenation over Co/Al 2O 3 catalysts prepared via a solid-state reaction of fine gibbsite and cobalt precursors. *Reac. Kinet. Mech. Cat.* 107 (1), 179–188. doi:10.1007/s11144-012-0459-8

Tarasov, A. L., Isaeva, V. I., Tkachenko, O. P., Chernyshev, V. V., and Kustov, L. M. (2018a). Conversion of CO_2 into liquid hydrocarbons in the presence of a Co-containing catalyst based on the microporous metal-organic framework MIL-53(Al). *Fuel Process. Technol.* 176, 101–106. doi:10.1016/j.fuproc.2018.03.016

Tarasov, A. L., Redina, E. A., and Isaeva, V. I. (2018b). Effect of the nature of catalysts on their properties in the hydrogenation of carbon dioxide. *Russ. J. Phys. Chem.* 92 (10), 1889–1892. doi:10.1134/s0036024418100345

Torrente-Murciano, L., Chapman, R. S. L., Narvaez-Dinamarca, A., Mattia, D., and Jones, M. D. (2016). Effect of nanostructured ceria as support for the iron catalysed hydrogenation of CO_2 into hydrocarbons. *Phys. Chem. Chem. Phys.* 18 (23), 15496–15500. doi:10.1039/c5cp07788e

Tursunov, O., and Tilyabaev, Z. (2019). Hydrogenation of CO_2 over Co supported on carbon nanotube, carbon nanotube-Nb2O5, carbon nanofiber, low-layered graphite fragments and Nb2O5. *J. Energy Inst.* 92 (1), 18–26. doi:10.1016/j.joei.2017.12.004

Visconti, C. G., Martinelli, M., Falbo, L., Fratalocchi, L., and Lietti, L. (2016). CO_2 hydrogenation to hydrocarbons over Co and Fe-based Fischer-Tropsch catalysts. *Catal. Today* 277, 161–170. doi:10.1016/j.cattod.2016.04.010

Visconti, C. G., Martinelli, M., Falbo, L., Infantes-Molina, A., Lietti, L., Forzatti, P., et al. (2017). CO_2 hydrogenation to lower olefins on a high surface area K-promoted bulk Fe-catalyst. *Appl. Catal. B Environ.* 200, 530–542. doi:10.1016/j.apcatb.2016.07.047

Wang, H., Hodgson, J., Shrestha, T. B., Thapa, P. S., Moore, D., Wu, X., et al. (2014). Carbon dioxide hydrogenation to aromatic hydrocarbons by using an iron/iron oxide nanocatalyst. *Beilstein J. Nanotechnol.* 5 (1), 760–769. doi:10.3762/bjnano.5.88

Wang, J., You, Z., Zhang, Q., Deng, W., and Wang, Y. (2013). Synthesis of lower olefins by hydrogenation of carbon dioxide over supported iron catalysts. *Catal. Today* 215, 186–193. doi:10.1016/j.cattod.2013.03.031

Wang, L., He, S., Wang, L., Lei, Y., Meng, X., and Xiao, F. S. (2019). Cobalt-nickel catalysts for selective hydrogenation of carbon dioxide into ethanol. *ACS Catal.* 9 (12), 11335–11340. doi:10.1021/acscatal.9b04187

Wang, L., Wang, L., Zhang, J., Liu, X., Wang, H., Zhang, W., et al. (2018). Selective hydrogenation of CO_2 to ethanol over cobalt catalysts. *Angew. Chem. Int. Ed.* 57 (21), 6104–6108. doi:10.1002/anie.201800729

Wang, S., Wu, T., Lin, J., Ji, Y., Yan, S., Pei, Y., et al. (2020). Iron-potassium on single-walled carbon nanotubes as efficient catalyst for CO_2 hydrogenation to heavy olefins. *ACS Catal.* 10 (11), 6389–6401. doi:10.1021/acscatal.0c00810

Wang, W., Jiang, X., Wang, X., and Song, C. (2018). Fe-Cu bimetallic catalysts for selective CO_2 hydrogenation to olefin-rich C2+ hydrocarbons. *Ind. Eng. Chem. Res.* 57 (13), 4535–4542. doi:10.1021/acs.iecr.8b00016

Wang, W., Wang, S., Ma, X., and Gong, J. (2011). Recent advances in catalytic hydrogenation of carbon dioxide. *Chem. Soc. Rev.* 40 (7), 3703–3727. doi:10.1039/c1cs15008a

Wang, X., Yang, G., Zhang, J., Chen, S., Wu, Y., Zhang, Q., et al. (2016). Synthesis of isoalkanes over a core (Fe-Zn-Zr)-shell (zeolite) catalyst by CO_2 hydrogenation. *Chem. Commun.* 52 (46), 7352–7355. doi:10.1039/c6cc01965j

Wang, X., Zeng, C. Y., Gong, N., Zhang, T., Wu, Y., Zhang, J., et al. (2021). Effective suppression of CO selectivity for CO_2 hydrogenation to high-quality gasoline. *ACS Catal.* 11 (3), 1528–1547. doi:10.1021/acscatal.0c04155

Wang, Y., Y., Kazumi, S., Gao, W., Gao, X., Li, H., Guo, X., et al. (2020). Direct conversion of CO_2 to aromatics with high yield via a modified Fischer-Tropsch synthesis pathway. *Appl. Catal. B Environ.* 269, 118792. doi:10.1016/j.apcatb.2020.118792

Wei, C., Tu, W., Jia, L., Liu, Y., Lian, H., Wang, P., et al. (2020). The evolutions of carbon and iron species modified by Na and their tuning effect on the hydrogenation of CO_2 to olefins. *Appl. Surf. Sci.* 525, 146622. doi:10.1016/j.apsusc.2020.146622

Wei, J., Ge, Q., Yao, R., Wen, Z., Fang, C., Guo, L., et al. (2017). Directly converting CO_2 into a gasoline fuel. *Nat. Commun.* 8, 15174–15178. doi:10.1038/ncomms15174

Wei, J., Sun, J., Wen, Z., Fang, C., Ge, Q., and Xu, H. (2016). New insights into the effect of sodium on Fe3O4- based nanocatalysts for CO_2 hydrogenation to light olefins. *Catal. Sci. Technol.* 6 (13), 4786–4793. doi:10.1039/c6cy00160b

Willauer, H. D., Ananth, R., Olsen, M. T., Drab, D. M., Hardy, D. R., and Williams, F. W. (2013). Modeling and kinetic analysis of CO_2 hydrogenation using a Mn and K-promoted Fe catalyst in a fixed-bed reactor. *J. CO2 Util.* 3–4, 56–64. doi:10.1016/j.jcou.2013.10.003

Wu, T., Lin, J., Cheng, Y., Tian, J., Wang, S., Xie, S., et al. (2018). Porous graphene-confined Fe-K as highly efficient catalyst for CO_2 direct hydrogenation to light olefins. *ACS Appl. Mat. Interfaces* 10 (28), 23439–23443. doi:10.1021/acsami.8b05411

Xie, C., Chen, C., Yu, Y., Su, J., Li, Y., Somorjai, G. A., et al. (2017). Tandem catalysis for CO_2 hydrogenation to C2-C4 hydrocarbons. *Nano Lett.* 17 (6), 3798–3802. doi:10.1021/acs.nanolett.7b01139

Xie, T., Wang, J., Ding, F., Zhang, A., Li, W., Guo, X., et al. (2017). CO_2 hydrogenation to hydrocarbons over alumina-supported iron catalyst: Effect of support pore size. *J. CO2 Util.* 19, 202–208. doi:10.1016/j.jcou.2017.03.022

Xu, Q., Xu, X., Fan, G., Yang, L., and Li, F. (2021). Unveiling the roles of Fe-Co interactions over ternary spinel-type ZnCoxFe2-xO4 catalysts for highly efficient CO_2 hydrogenation to produce light olefins. *J. Catal.* 400, 355–366. doi:10.1016/j.jcat.2021.07.002

Xu, Y., Shi, C., Liu, B., Wang, T., Zheng, J., Li, W., et al. (2019). Selective production of aromatics from CO_2. *Catal. Sci. Technol.* 9 (3), 593–610. doi:10.1039/c8cy02024h

Yao, R., Wei, J., Ge, Q., Xu, J., Han, Y., Xu, H., et al. (2021). Structure sensitivity of iron oxide catalyst for CO_2 hydrogenation. *Catal. Today* 371, 134–141. doi:10.1016/j.cattod.2020.07.073

Yao, Y., Liu, X., Hildebrandt, D., and Glasser, D. (2012). The effect of CO_2 on a cobalt-based catalyst for low temperature Fischer-Tropsch synthesis. *Chem. Eng. J.* 193–194, 318–327. doi:10.1016/j.cej.2012.04.045

You, Z., Deng, W., Zhang, Q., and Wang, Y. (2013). Hydrogenation of carbon dioxide to light olefins over non-supported iron catalyst. *Chin. J. Catal.* 34 (5), 956–963. doi:10.1016/S1872-2067(12)60559-2

Yuan, F., Zhang, G., Zhu, J., Ding, F., Zhang, A., Song, C., et al. (2021). Boosting light olefin selectivity in CO_2 hydrogenation by adding Co to Fe catalysts within close proximity. *Catal. Today* 371, 142–149. doi:10.1016/j.cattod.2020.07.072

Zhang, J., Lu, S., Su, X., Fan, S., Ma, Q., and Zhao, T. (2015). Selective formation of light olefins from CO_2 hydrogenation over Fe-Zn-K catalysts. *J. CO2 Util.* 12, 95–100. doi:10.1016/j.jcou.2015.05.004

Zhang, J., Su, X., Wang, X., Ma, Q., Fan, S., and Zhao, T. S. (2018). Promotion effects of Ce added Fe–Zr–K on CO_2 hydrogenation to light olefins. *Reac. Kinet. Mech. Cat.* 124 (2), 575–585. doi:10.1007/s11144-018-1377-1

Zhang, S., Liu, X., Shao, Z., Wang, H., and Sun, Y. (2020). Direct CO_2 hydrogenation to ethanol over supported Co_2C catalysts: Studies on support effects and mechanism. *J. Catal.* 382, 86–96. doi:10.1016/j.jcat.2019.11.038

Zhang, Z., Huang, G., Tang, X., Yin, H., Kang, J., Zhang, Q., et al. (2022a). Zn and Na promoted Fe catalysts for sustainable production of high-valued olefins by CO_2 hydrogenation. *Fuel* 309, 122105. doi:10.1016/j.fuel.2021.122105

Zhang, Z., Liu, Y., Jia, L., Sun, C., Chen, B., Liu, R., et al. (2022b). Effects of the reducing gas atmosphere on performance of FeCeNa catalyst for the hydrogenation of CO_2 to olefins. *Chem. Eng. J.* 428, 131388. doi:10.1016/j.cej.2021.131388

Zhang, Z., Wei, C., Jia, L., Liu, Y., Sun, C., Wang, P., et al. (2020). Insights into the regulation of FeNa catalysts modified by Mn promoter and their tuning effect on the hydrogenation of CO_2 to light olefins. *J. Catal.* 390, 12–22. doi:10.1016/j.jcat.2020.07.020

Zhao, H., Guo, L., Gao, W., Chen, F., Wu, X., Wang, K., et al. (2021). Multi-promoters regulated iron catalyst with well-matching reverse water-gas shift and chain propagation for boosting CO_2 hydrogenation. *J. CO2 Util.* 52, 101700. doi:10.1016/j.jcou.2021.101700

Zheng, Y., Xu, C., Zhang, X., Wu, Q., and Liu, J. (2021). Synergistic effect of alkali na and k promoter on fe-co-cu-al catalysts for CO_2 hydrogenation to light hydrocarbons. *Catalysts* 11 (6), 735. doi:10.3390/catal11060735